ANL-6773

Argonne National Laboratory

ANALYTICAL STUDY OF THE TRANSFER FUNCTION OF EBR-I MARK IV

by

Jiro Wakabayashi

Price $1.50 . *Available from the Office of Technical Services, Department of Commerce, Washington 25, D.C.*

ANL-6773
Reactor Technology
(TID-4500, 26th Ed.)
AEC Research and
Development Report

ARGONNE NATIONAL LABORATORY
9700 South Cass Avenue
Argonne, Illinois 60440

ANALYTICAL STUDY OF THE TRANSFER FUNCTION OF EBR-I MARK IV

by

Jiro Wakabayashi*

Idaho Division

*Engineering Research Institute,
Kyoto University, Kyoto, Japan

September 1963

Operated by The University of Chicago
under
Contract W-31-109-eng-38
with the
U. S. Atomic Energy Commission

TABLE OF CONTENTS

LIST OF FIGURES

LIST OF TABLES

ANALYTICAL STUDY OF THE TRANSFER FUNCTION OF EBR-I MARK IV

Jiro Wakabayashi

I. INTRODUCTION

The dynamic behavior of liquid metal-cooled fast reactors for small perturbations was investigated in a systematic way. Since the reactivity coefficients of fast reactors due to temperature are small compared with those of thermal reactors, certain feedback mechanisms which must be taken into consideration in the transfer function analysis of thermal systems may be neglected.

In this report the following feedback mechanisms are analyzed theoretically:

1. the reactivity feedback due to axial expansion of a fuel slug;
2. the reactivity feedback due to radial expansion of a fuel slug. The coolant volume in the core may be changed by this expansion;
3. the reactivity effect due to cladding expansion. The reactivity is changed for the same reason as for item 2;
4. the reactivity effect due to coolant expansion in the core;
5. the reactivity effect due to coolant expansion in the blanket;
6. the reactivity effect due to axial expansion of a blanket slug;
7. the reactivity effect due to bowing of a fuel slug in the jacket;
8. the reactivity effect due to expansion of a fuel-assembly tube.

The numerical analysis was done for the EBR-I Mark IV, and the results of the analysis showed a good agreement with those of experiment.

Since the analysis was done theoretically it is expected that the estimation of transfer functions of the liquid metal-cooled fast reactors may be done with sufficient accuracy by a similar procedure during the designing period.

II. ASSUMPTIONS IN THE ANALYSIS

For simplicity the following assumptions were made in the analysis:

1. Since the reactor core is sufficiently small, the dynamic behavior of the reactor is spatially independent.

2. In the transfer function study, the power response due to the small reactivity oscillation is investigated. The amplitude of the power oscillation is so small that (i) the nonlinear effect of the neutron chain reaction and the nonlinearity of the heat transfer may be ignored and (ii) the spatial power deviation will be proportional to the initial power distribution.

3. The reactivity effect due to the local temperature is proportional to the product of the local temperature deviation and the local power.

4. The radial fission distribution in a single fuel slug is constant, i.e., the power generation rate in a single fuel rod is radially uniform.

5. Since the ratio of the power generation at the core wall to the core center at the same elevation is nearly equal to 0.7, the effect of the radial power distribution in the core will not be important in the transfer function study, and this effect may be ignored in the analysis.

6. Inasmuch as the upper and lower blanket power is very small compared with the core power, the upper and lower blanket power may be ignored in the analysis.

7. Since the inner blanket power is very small compared with the core power, the reactivity effect due to the inner blanket temperature may be ignored in the analysis. Only the effect of the temperature deviation of the coolant at the core inlet due to the preheating in the inner blanket is introduced in the analysis as the effect of the inner blanket.

8. The ratio of power generation in the core, inner blanket, and outer blanket are 80%, 5%, and 15% of total power, respectively. The outer blanket power has no effect on the dynamic behavior of the reactor.

9. From the experimental data the axial power distribution in the core has sinusoidal form.

10. According to assumption 7, the spatial power distribution in the inner blanket may be ignored in the analysis of the outlet coolant temperature of the inner core.

11. Since the temperature difference between the NaK bond and Zircaloy cladding is sufficiently small compared with the temperature difference between the Zircaloy cladding and the NaK coolant, the NaK bond and the Zircaloy cladding can be treated together.

12. The reactivity change due to bowing of a fuel slug may be replaced by the reactivity change due to the change in the core radius.

13. From assumption 2, the spatial temperature distribution in the core or upper blanket will remain constant. Then the temperature difference across the fuel slug or blanket slug in the radial direction of the core will be proportional to the temperature of the fuel slug or blanket slug respectively.

14. Since the neutron energy in the core is rather high, the Doppler effect is negligible.

15. The radial expansion of a fuel rod will be absorbed by the tightening rod spring and will not affect the radial displacement of the core.

III. ZERO-POWER REACTOR TRANSFER FUNCTION

From assumption 1, the kinetic characteristics of the reactor may be obtained by solving the following spatially independent kinetic equations (see Appendix G for the meaning of symbols):

$$\frac{dN}{dt} = \frac{\rho - \beta}{\ell^*} N + \Sigma \lambda_i C_i \quad ; \tag{3.1}$$

$$\frac{dC_i}{dt} = \frac{\beta_i}{\ell^*} N - \lambda_i C_i \quad ; \tag{3.2}$$

$$\beta = \sum_{i=1}^{6} \beta_i \quad ; \quad i = 1,2,\ldots,6 \quad ;$$

$$\rho = \rho_{ex} + \rho_f \quad , \tag{3.3}$$

where ρ_{ex} and ρ_f are the externally inserted reactivity and the feedback reactivity, respectively. The values of λ_i and β_i are given in Table 3.1.[1]

From assumption 2, the transfer function of the zero-power reactor is denoted as follows:

$$\frac{N(s)/N_0}{\rho(s)} = \frac{1/\ell^*}{s\left[1 + \sum_{i=1}^{6} \frac{\beta_i}{\ell^*(s + \lambda_i)}\right]} \quad . \tag{3.4}$$

Table 3.1

VALUES OF λ_i AND β_i

i	λ_i	β_i
1	0.0129	0.0000918
2	0.0311	0.0007193
3	0.1340	0.0005979
4	0.3310	0.0010182
5	1.2600	0.0003996
6	3.2100	0.0001332

$\Sigma\beta_i = 0.00296$; $\ell^* = 4 \times 10^{-8}$ sec

IV. POWER GENERATION TO CORE TEMPERATURE TRANSFER FUNCTION

From assumption 11, the NaK bond and the Zircaloy cladding will be treated as one medium having a single heat capacity and a single thermal resistance. If the single thermal resistance is equal to the thermal resistance of the layer of NaK bond and cladding, the temperature of this medium can be given by the approximate value of the cladding surface temperature, and it can be assumed that the NaK bond temperature is nearly equal to the cladding surface temperature.

According to assumption 4, the temperature in the fuel slug of radius R_1, thermal conductivity λ_f, and diffusivity k_f may be obtained by solution of the equation

$$\nabla^2\theta_f + \frac{\dot{Q}_g/\pi R_1^2}{\lambda_f} = \frac{1}{k_f}\frac{d\theta_f}{dt} \quad . \tag{4.1}$$

Since the fuel slug is cylindrical, the boundary conditions are:

$$-\left.\frac{\partial\theta_f(r,t)}{\partial r}\right|_{R_1} = \frac{H_1}{\lambda_f}\left\{\theta_f(r,t) - \theta_c(t)\right\} \quad ; \tag{4.2}$$

$$\theta_f(0,t) \neq \infty \quad . \tag{4.3}$$

By using the Laplace transform method and substituting the following relations:

$$\dot{Q}_c = \left\{\theta_f(R,s) - \theta_c(s)\right\} 2\pi R_1 H_1 \quad ; \tag{4.4}$$

$$M \equiv R_1 H_1 / \lambda_f \quad ; \tag{4.5}$$

$$T \equiv R_1^2 / k_f \quad , \tag{4.6}$$

we obtain

$$\dot{Q}_c(s) = \left\{ \dot{Q}_g(s) - C_f s \theta_c(s) \right\} \left[\frac{2 I_1(\sqrt{Ts}) / \sqrt{Ts}}{I_0(\sqrt{Ts}) + \frac{\sqrt{Ts}}{M} I_1(\sqrt{Ts})} \right]$$

$$= \left\{ \dot{Q}_g(s) - C_f s \theta_c(s) \right\} \sum_{i=1}^{\infty} \frac{F_i}{1 + \tau_i s} \quad , \tag{4.7}$$

where F_i and τ_i are found from the simultaneous solution of

$$F_i = \frac{4\tau_i / T}{1 + (T / \tau_i M^2)} \tag{4.8}$$

and

$$\tau_i = \sqrt{T / \tau_i} \left[\frac{J_1(\sqrt{T / \tau_i})}{J_0(\sqrt{T / \tau_i})} \right] \quad . \tag{4.9}$$

From the numerical calculation, it is found that F_i and τ_i are very small at $i > 2$. Eq. (4.7) may therefore be rewritten as follows:

$$\dot{Q}_c(s) \simeq \{ \dot{Q}_g(s) - C_f s \theta_c(s) \} \left\{ \frac{F_1}{1 + \tau_1 s} + \frac{\tilde{F}_2}{1 + \tilde{\tau}_2 s} \right\} \quad , \tag{4.10}$$

where

$$\tilde{\tau}_2 = \frac{\sum_{i=2}^{\infty} F_i \tau_i / T}{\sum_{i=2}^{\infty} F_i / T} \quad ; \quad \tilde{F}_2 = 1 - F_1 \quad . \tag{4.11}$$

Since a certain fraction γ of power generation is carried by gamma radiation and is released in the coolant directly, Eq. (4.10) may be re-written as

$$\dot{Q}_c(s) = \{ (1 - \gamma) \dot{Q}_g(s) - C_f s \theta_c(s) \} \left\{ \frac{F_1}{1 + \tau_1 s} + \frac{\tilde{F}_2}{1 + \tilde{\tau}_2 s} \right\} \quad . \tag{4.12}$$

The fuel rod temperature, NaK bond and cladding temperature, and coolant temperature are found by solving the following equations:

$$C_f\, s\theta_f(\chi, s) = (1-\gamma)\,\dot{Q}_g(\chi, s) - \dot{Q}_c(\chi, s) \quad ; \tag{4.13}$$

$$C_c\, s\theta_c(\chi_i, s) = \dot{Q}_c(\chi, s) - \{\dot{Q}_n(\chi, s) - \gamma\,\dot{Q}_g(\chi, s)\} \quad ; \tag{4.14}$$

$$\dot{Q}_n(\chi, s) - \gamma\,\dot{Q}_g(\chi, s) = 2\pi R_2 H_2\, \{\theta_c(\chi, s) - \theta_n(\chi, s)\} \quad ; \tag{4.15}$$

$$\dot{Q}_n(\chi, s) = C_n s\,\theta_n(\chi, s) + vC_n \frac{d\theta_n(\chi, s)}{d\chi} \quad . \tag{4.16}$$

From Eqs. (4.12) through (4.16) (see Appendix A), $\theta_f(\chi, s)$, $\theta_c(\chi, s)$, and $\theta_n(\chi, s)$ are

$$\theta_f(\chi, s) = \dot{Q}_g(\chi, s)\,(1-\gamma)\left\{\frac{1}{C_f s} - \xi(s)\left(\frac{1}{C_f s} + \frac{C_c}{2\pi R_2 H_2 C_f}\right)\right\} + \xi(s)\,\theta_n(\chi, s) \quad ; \tag{4.17}$$

$$\theta_c(\chi, s) = \frac{\xi(s)(1-\gamma)}{2\pi R_2 H_2}\,\dot{Q}_g(\chi, s) + \xi(s)\,\frac{\theta_n(\chi, s)}{F(s)} \quad ; \tag{4.18}$$

$$\theta_n(\chi, s) = \{\gamma + (1-\gamma)\xi(s)\}\,\frac{1}{vC_n}\int_0^{\chi} \dot{Q}_g(\chi', s)\, e^{\eta(s)(\chi' - \chi)}\, d\chi' + \theta_{nin}(s)\, e^{-\frac{\chi}{v}s} \quad , \tag{4.19}$$

where

$$\xi(s) = \frac{F(s)}{1 + \dfrac{s}{2\pi R_2 H_2}\,\{C_c + C_f\, F(s)\}} \tag{4.20}$$

$$\eta(s) = \frac{s}{v}\left[1 + \frac{\{C_c + C_f\, F(s)\}/C_n}{1 + \dfrac{s}{2\pi R_2 H_2}\,\{C_c + C_f\, F(s)\}}\right] \quad ; \tag{4.21}$$

$$F(s) = \frac{F_1}{1 + \tau_1 s} + \frac{\tilde{F}_2}{1 + \tilde{\tau}_2 s} \quad . \tag{4.22}$$

Experimental data and assumption 5 give the power generation rate in the core as

$$\dot{Q}_g(\chi, t) = \dot{Q}_g(t)\, D(\chi) \quad , \tag{4.23}$$

where

$$D(\chi) = A \sin (B\chi + C) \tag{4.24}$$

and

$$\frac{1}{L} \int_0^L D(\chi)\, d\chi = 1 \quad . \tag{4.25}$$

From assumption 10, the power generation rate in the inner blanket will be

$$_b\dot{Q}_g(\chi, t) = {}_b\dot{Q}_g(t) \quad . \tag{4.26}$$

If the coolant transport time from the inner blanket outlet to the core center is denoted as T_r, the simplified transfer functions of the power generation rate to the core temperatures are given as follows (see Appendix B):

$$\frac{\bar{\theta}_n(s)}{\dot{Q}_g(s)} = \frac{(1 + \tau_8 s)(1 + \tau_3 s)(1 + \tau_4 s)}{(1 + \tilde{\tau}_2 s)(1 + \alpha_1 s + \alpha_2 s^2 + \alpha_3 s^3)} \frac{\bar{A}_1 \left\{\bar{C}_1 + \bar{C}_2 s + \bar{C}_3 s^2\right\}}{(1 + \tau_3 s)(1 + \tau_4 s)}$$

$$+ \frac{\bar{A}_1 \left\{\bar{C}_4 + \bar{C}_5 s + \bar{C}_6 s^2 + \bar{C}_7 s^3 + \bar{C}_8 s^4\right\}}{(1 + \beta_1 s + \beta_2 s^2)(1 + \gamma_1 s + \gamma_2 s^2 + \gamma_3 s^3)}$$

$$+ \frac{{}_b\dot{Q}_g(s)}{\dot{Q}_g(s)} \frac{{}_b\theta_n({}_bL, s)}{{}_b\dot{Q}_g(s)} \frac{1}{1 + T_r s} \quad ; \tag{4.27}$$

$$\frac{\bar{\theta}_c(s)}{\dot{Q}_g(s)} \simeq \frac{\bar{B}_1 (1 + \tau_5 s)}{(1 + \tilde{\tau}_2 s)(1 + \tau_3 s)(1 + \tau_4 s)} + \frac{(1 + \tau_1 s)}{(1 + \tau_3 s)(1 + \tau_4 s)} \frac{\bar{\theta}_n(s)}{\dot{Q}_g(s)} \quad ; \tag{4.28}$$

$$\frac{\bar{\theta}_f(s)}{\dot{Q}_g(s)} \simeq \bar{B}_2 \frac{\bar{B}_3 + \bar{B}_4 s + \bar{B}_5 s^2}{(1 + \tilde{\tau}_2 s)(1 + \tau_3 s)(1 + \tau_4 s)} + \frac{1}{(1 + \tau_3 s)(1 + \tau_4 s)} \frac{\bar{\theta}_n(s)}{\dot{Q}_g(s)} \quad , \tag{4.29}$$

where

$$\frac{{}_b\theta_n({}_bL,s)}{{}_b\dot{Q}_g(s)} \simeq \frac{(1 + {}_b\tau_8 s)\ {}_bL/({}_bC_n\ {}_bv)}{(1 + {}_b\tilde{\tau}_2 s)\left\{(1 + {}_b\tau_3 s)(1 + {}_b\tau_4 s) + \frac{{}_b\tau_0 s}{2}(1 + {}_b\tau_6 s)(1 + {}_b\tau_7 s)\right\}} \quad . \tag{4.30}$$

V. POWER GENERATION TO UPPER BLANKET TEMPERATURE TRANSFER FUNCTIONS

From assumption 6, the temperatures of the upper blanket are dependent upon the coolant which was preheated in the core.

Since the reactivity effects due to the cladding and NaK bond temperatures will be ignored, the blanket slug, NaK bond, and cladding may be treated as one medium having a single heat capacity and a single thermal resistance. The effective heat transfer coefficient of the blanket slug to coolant is then calculated as follows:

$${}_uH_2 = \frac{1}{(\delta_{Na}/\lambda_{Na}) + (\delta_{Zr}/\lambda_{Zr}) + (1/H_2)} = \frac{1}{(1/H_1) + (1/H_2)} \quad . \tag{5.1}$$

The coolant and blanket rod temperatures are

$${}_uC_f\, s\, {}_u\theta_f(\chi,s) = {}_uH_2\left\{{}_u\theta_n(\chi,s) - {}_u\theta_f(\chi,s)\right\} 2\pi R_2 \quad ; \tag{5.2}$$

$${}_uC_n\, s\, {}_u\theta_n(\chi,s) = -{}_uH_2\left\{{}_u\theta_n(\chi,s) - {}_u\theta_f(\chi,s)\right\} 2\pi R_2$$

$$- {}_uv\ {}_uC_n \frac{d_u\theta_n(\chi,s)}{d\chi} \quad . \tag{5.3}$$

Solving Eqs. (5.2) and (5.3), we obtain

$${}_u\theta_n(\chi,s) = K e^{-\psi(s)\chi} \quad ; \tag{5.4}$$

$${}_u\theta_f(\chi,s) = \frac{1}{1 + \frac{{}_uC_f s}{2\pi R_2\, {}_uH_2}}\ {}_u\theta_n(\chi,s) \quad , \tag{5.5}$$

where

$$\psi(s) = \frac{{}_uH_2}{{}_uC_n\ {}_uv}\left\{\frac{{}_uC_n}{2\pi R_2\ {}_uH_2}\ s + 1 - \frac{1}{1 + \frac{{}_uC_f\ s}{2\pi R_2\ {}_uH_2}}\right\} \quad ; \tag{5.6}$$

$$K = \theta_n(L,s)$$

$$= \left\{\gamma + (1-\gamma)\xi(s)\right\}\frac{\dot{Q}_g(s)\ A}{vC_n\ B}\left[\frac{\frac{\eta(s)}{B}\sin(BL + C) - \cos(BL + C)}{1 + \left\{\frac{\eta(s)}{B}\right\}^2}\right.$$

$$\left. - \frac{e^{-\eta(s)L}\left\{\frac{\eta(s)}{B}\sin C - \cos C\right\}}{1 + \left\{\frac{\eta(s)}{B}\right\}^2}\right] + {}_b\theta_n(L_b s)\ \frac{1}{1 + T'_r\ s} \tag{5.7}$$

The average values of ${}_u\theta_f(\chi, s)$ and ${}_u\theta_n(\chi, s)$ will be

$${}_u\bar{\theta}_f(s) = \frac{1}{1 + \frac{{}_uC_f\ s}{2\pi R_2\ {}_uH_2}}\ {}_u\bar{\theta}_n(s) \quad ; \tag{5.8}$$

$${}_u\bar{\theta}_n(s) = \frac{K}{\psi(s)}\left(1 - e^{-\psi(s)\,{}_uL}\right) \simeq \frac{\theta_n(L,s)}{1 + \frac{\psi(s)}{2}\ {}_uL} \quad . \tag{5.9}$$

The power generation rate to upper blanket temperature transfer functions may be simplified as follows (see Appendix C):

$$\frac{{}_u\bar{\theta}_f(s)}{\dot{Q}_g(s)} = \frac{1}{1 + \tau_{12}s}\ \frac{{}_u\bar{\theta}_n(s)}{\dot{Q}_g(s)} \quad ; \tag{5.10}$$

$$\frac{{}_u\theta_n(s)}{\dot{Q}_g(s)} = \frac{(1 + \tau_8 s)}{(1 + \tilde{\tau}_2 s)(1 + \alpha_1 s + \alpha_2 s^2 + \alpha_3 s^3)}\ \frac{A}{v\ C_n\ B}$$

$$\frac{\bar{D}_6 + \bar{D}_7 s + \bar{D}_8 s^2 + \bar{D}_9 s^3 + \bar{D}_{10} s^4}{1 + \beta_1 s + \beta_2 s^2}\ \frac{1 + \tau_{12}s}{1 + \bar{E}_1 s + \bar{E}_2 s^2} \quad . \tag{5.11}$$

VI. POWER GENERATION RATE TO CORE RADIAL DISPLACEMENT (DUE TO FUEL BOWING) TRANSFER FUNCTION

Since the fuel rods are held rigid by tightening rods and ribs, it is assumed that the fuel rods are not bent as a result of the radial temperature difference in the core. However, fuel slugs may be bent as a result of the radial temperature difference in the core because there are thin NaK bonds between the fuel slug and jacket. The fuel slugs also have four ribs, but there is an approximately 0.0127-cm clearance between the ribs and jacket. Since the location of fuel slug ribs are random, the mean value of clearance between the ribs and jacket may be assumed to be $0.0127 \times 4/\pi \log (1 \times \sqrt{2}) \simeq 0.01425$ cm. The depleted uranium slugs which are used in the upper and lower blanket do not have ribs, and the clearance between the depleted uranium slug and jacket may be assumed to be 0.032 cm.

The bowing of the fuel slug or blanket slug may occur in the radial direction of the core. Since the locations of fuel slug and blanket slug are random, the maximum clearances involved in the bending of the fuel slug or blanket slug are 0.0285 cm or 0.064 cm, respectively. The minimum clearance is, of course, 0 cm. The centers of the fuel slug or blanket slug are usually not located on the line of the core center to the jacket center. This fact denotes a decrease of clearance for the fuel slug or blanket slug, and, for convenience, the effect of this decrease may be indicated by a multiplication factor of 1/2.

Also for convenience, the temperature difference across the fuel slug or upper blanket slug is assumed to be constant in the axial direction. With this assumption and with the condition that the slugs do not touch the inside wall of the jacket, the following equations are obtained:

$$\frac{d^2 r_1}{d\chi^2} = -\frac{\alpha \theta_{df}}{d} \quad \text{in the core } (0 < \chi \leq L) \quad ; \tag{6.1}$$

$$\frac{d^2 r_1}{d\chi^2} = -\frac{u\alpha \, u\theta_{df}}{d} \quad \text{in the upper blanket } (L \leq \chi \leq L + {}_uL) \quad . \tag{6.2}$$

The boundary conditions of Eq. (6.1) and (6.2) are as follows:

$r_1 = 0$ at $\chi = 0$ and $\chi = L + {}_uL$;

r_1 and $\frac{dr_1}{d\chi}$ are continuous at $\chi = L$.

The solutions of the Eqs. (6.1) and (6.2) may be written as follows:

$$r_1 = -\frac{\alpha\theta_{df}}{2d}\chi^2 + \overline{N}_1\chi \quad \text{at } 0<\chi<L \quad ; \tag{6.3}$$

$$r_1 = -\frac{{}_u\alpha_u\theta_{df}}{2_{ud}}\chi^2 + \overline{N}_2\chi + \overline{N}_3 \quad \text{at } L<\chi<L+{}_uL \quad , \tag{6.4}$$

where

$$\overline{N}_1 = \frac{\alpha\theta_{df}L}{d}\left[\frac{(\alpha\theta_{df} - {}_u\alpha_u\theta_{df})}{\alpha\theta_{df}}\left\{1 - \frac{L}{2\,(L+{}_uL)}\right\} + \frac{{}_u\alpha_u\theta_{df}}{2\,\alpha\theta_{df}}\,\frac{(L+{}_uL)}{L}\right] \quad ; \tag{6.5}$$

$$\overline{N}_2 = \frac{\alpha\theta_{df}L}{d}\left[\frac{{}_u\alpha_u\theta_{df}}{2\,\alpha\theta_{df}}\,\frac{(L+{}_uL)}{L} - \frac{(\alpha\theta_{df} - {}_u\alpha_u\theta_{df})}{2\,\alpha\theta_{df}}\left(\frac{L}{L+{}_uL}\right)\right] \quad ; \tag{6.6}$$

$$\overline{N}_3 = \frac{\alpha\theta_{df}L^2}{d}\,\frac{(\alpha\theta_{df} - {}_u\alpha_u\theta_{df})}{2\,\alpha\theta_{df}} \quad . \tag{6.7}$$

Assuming that the reactivity change due to bowing of the fuel slug has the same weighting function as that of the temperature difference, the effective displacement of the fuel slug due to bowing will be

$$\overline{r}_1(s) = \frac{1}{L}\int_0^L r_1(\chi, s)\, A \sin(B\chi + C)\, d\chi$$

$$= -\frac{\alpha\theta_{df}(s)L^2A}{2d}\left\{\frac{2}{B^2L^2}\sin(BL+C) - \left(\frac{1}{BL} - \frac{2}{B^3L^3}\right)\cos(BL+C) - \frac{2}{B^3L^3}\cos C\right\}$$

$$+ \overline{N}_1LA\left\{\frac{1}{B^2L^2}\sin(BL+C) - \frac{1}{BL}\cos(BL+C) - \frac{1}{B^2L^2}\sin C\right\} \quad . \tag{6.8}$$

According to assumption 13, $\theta_{df}(s)$ and ${}_u\theta_{df}(s)$ are proportional to $\overline{\theta}'_f(s)$ and ${}_u\overline{\theta}_f(s)$, respectively. Now $\overline{\theta}'_f(s)$ is given as (see Appendix D)

$$\bar{\theta}'_f(s) = \frac{1}{L}\int_0^L \theta_f(\chi,s)\,d\chi$$

$$\simeq \frac{(1-\gamma)\dot{Q}_g(s)}{C_f}\,\frac{\bar{B}_3 + \bar{B}_4 s + \bar{B}_5 s^2}{(1+\tilde{\tau}_2 s)(1+\tau_3 s)(1+\tau_4 s)}$$

$$+\frac{\dot{Q}_g(s)}{vC_nB}\,\frac{(1+\tau_8 s)}{(1+\tilde{\tau}_2 s)(1+\alpha_1 s+\alpha_2 s^2+\alpha_3 s^3)}$$

$$\cdot\left[\frac{(1+\tau_5 s)(\bar{F}_2+\bar{F}_4 s+\bar{F}_5 s^2)}{(1+\tilde{\tau}_2 s)(1+\tau_3 s)(1+\tau_4 s)} + \frac{\bar{F}_3(1+\tau_5 s)\{1+(\tau_3+\tau_4)s+\tau_3\tau_4 s^2\}}{(1+\tilde{\tau}_2 s)(1+\beta_1 s+\beta_2 s^2)}\right]. \tag{6.9}$$

Eqs. (5.11), (5.12),(6.9), and assumption 13 show that the ratio of ${}_u\theta_{df}$ and θ_{df} at the steady state is constant and independent of the steady-state power. The deviation of fuel-slug displacement is therefore proportional to the deviation of average fuel-slug temperature.

The condition that each slug does not touch the jacket wall is given by the following equation, because the clearance between the blanket slug and jacket wall is very large compared with the clearance between the fuel slug and jacket.

$$\frac{\theta_n(Ls)}{\dot{Q}_g(s)} \simeq \frac{(1+\tau_8 s)}{(1+\tilde{\tau}_2 s)(1+\tau_3 s)(1+\tau_4 s)}\,\frac{A}{vC_nB}\,\frac{1}{1+\left\{\tau_{10}s\,\frac{(1+\tau_0 s)(1+\tau_7 s)}{(1+\tau_3 s)(1+\tau_4 s)}\right\}^2}$$

$$\times\left[s\,\frac{(1+\tau_6 s)(1+\tau_7 s)}{(1+\tau_3 s)(1+\tau_4 s)}\,\bar{D}_1\left\{\bar{D}_2 + \frac{\bar{D}_3}{1+\tau_0 s\,\frac{(1+\tau_6 s)(1+\tau_7 s)}{(1+\tau_3 s)(1+\tau_4 s)}}\right\} + \bar{D}_4 + \frac{\bar{D}_5}{1+\tau_0 s\,\frac{(1+\tau_6 s)(1+\tau_7 s)}{(1+\tau_3 s)(1+\tau_4 s)}}\right] + \frac{b\dot{Q}_g(s)}{\dot{Q}_g(s)}\,\frac{b\theta_n(bLs)}{b\dot{Q}_g(s)}\,\frac{1}{1+T'_r s} \tag{6.10}$$

$$\simeq \frac{(1+\tau_8 s)(1+\tau_3 s)(1+\tau_4 s)}{(1+\tilde{\tau}_2 s)(1+\alpha_1 s+\alpha_2 s^2+\alpha_3 s^3)}\,\frac{(A/vC_nB)\{\bar{D}_6+\bar{D}_7 s+\bar{D}_8 s^2+\bar{D}_9 s^3+\bar{D}_{10}s^4\}}{(1+\beta_1 s+\beta_2 s^2)(1+\tau_3 s)(1+\tau_4 s)}, \tag{6.11}$$

The condition represented by Eq. (6.10) or (6.11) may be satisfied at the steady-state power level of less than P_{1m}, P_{2m}, and P_{3m} for flow rates of 291 gpm, 200 gpm, and 100 gpm, respectively.

If a fuel slug touches the jacket wall, the bowing of the fuel slug might have little effect on the deviation of average fuel-slug displacement, because, when a fuel slug touching the jacket bows toward the core center,

the ends of the slug will displace the adjacent slugs above and below it in the opposite direction, and this effect and the bowing effect tend to cancel each other.

At the flow rate of 291 gpm and the steady-state power level P_1, the proportion of the fuel slug that does not touch the jacket wall may be considered as $(P_{1m} - P_1)/P_{1m}$ at $P_1 < P_{1m}$ or 0 at $P_1 > P_{1m}$. Similar relations may be obtained at different flow rates.

From the reasons mentioned above, the transfer function of power generation to fuel rods displacement is as follows:

$$\frac{\bar{r}_1(s)}{\dot{Q}_g(s)} = \frac{\bar{\theta}_f'(s)}{\dot{Q}_g(s)} \frac{(P_{im} - P_i)}{P_{im}} \bar{G}_1 \quad , \tag{6.12}$$

where i is 1, 2, or 3 corresponding to the flow rate of 291 gpm, 200 gpm or 100 gpm, respectively,

$$\frac{\bar{\theta}_f'(s)}{Q_g(s)} = \frac{(1-\gamma)}{C_f \bar{B}_2} \left[\frac{\bar{B}_2(\bar{B}_3 + \bar{B}_4 s + \bar{B}_5 s^2)}{(1+\tilde{\tau}_2 s)(1+\tau_3 s)(1+\tau_4 s)} + \frac{\bar{B}_2/vC_nB}{1-\gamma} \right.$$

$$\cdot \frac{1+\tau_8 s}{(1+\tilde{\tau}_2 s)(1+\alpha_1 s+\alpha_2 s^2+\alpha_3 s^3)} \left\{ \frac{(1+\tau_5 s)(\bar{F}_2 + \bar{F}_4 s + \bar{F}_5 s^2)}{(1+\tilde{\tau}_2 s)(1+\tau_3 s)(1+\tau_4 s)} \right.$$

$$\left. \left. + \frac{\bar{F}_3(1+\tau_5 s)\{1+(\tau_3+\tau_4)s+\tau_3\tau_4 s^2\}}{(1+\tilde{\tau}_2 s)(1+\beta_1 s+\beta_2 s^2)} \right\} \right] \quad ; \tag{6.13}$$

$$\bar{G}_1 = \frac{\alpha L^2 A}{2d} \frac{\theta_{df}(s)}{\bar{\theta}_f'(s)} \left[\left\{ \frac{-1}{B^2L^2} \sin(BL+C) \right. \right.$$

$$+ \left(\frac{1}{2\,BL} - \frac{1}{B^3L^3} \right) \cos(BL+C) + \frac{1}{B^2L^2} \cos C \Big\}$$

$$+ \left\{ \left(1 - \frac{u\alpha_u \bar{\theta}_f}{\alpha \bar{\theta}_f'} \right) \left\{ 1 - \frac{L}{2(L+{}_uL)} \right\} + \frac{u\alpha_u \bar{\theta}_f}{2\alpha \bar{\theta}_f} \frac{(L+{}_uL)}{L} \right\}$$

$$\left. \left\{ \frac{1}{L^2B^2} \sin(BL+C) - \frac{1}{BL} \cos(BL+C) - \frac{1}{B^2L^2} \sin C \right\} \right] \quad ; \tag{6.14}$$

$$\frac{\theta_{df}(s)}{\bar{\theta}_f'(s)} = \frac{u\theta_{df}(s)}{u\bar{\theta}_f(s)} = d\bar{G}_2 \quad . \tag{6.15}$$

The constant $\overline{G}_2$ is given by

$$\overline{G}_2 = \frac{\text{(fuel- or blanket-slug temperature gradient for the radial direction of core)}}{\text{(average fuel or blanket slug temperature)}} \quad (6.16)$$

From assumption 2, the radial temperature distribution in the core is similar to the radial power distribution. Since the upper blanket-slug temperature is dependent upon the coolant which was preheated in the core, the radial temperature distribution in the upper blanket is also similar to the radial power distribution in the core. The constant $\overline{G}_2$ is, therefore, obtained from the experimental data for the fission spectrum in the core.

VII. POWER GENERATION RATE TO CORE RADIAL DISPLACEMENT (DUE TO THERMAL EXPANSION) TRANSFER FUNCTION

Since the core and blanket assemblies are held by the core clamp, the pressure of the contacting surfaces of any neighboring two hexagonal tubes is balanced. If the hexagonal tubes in the core expand radially due to temperature rise, the hexagonal tube in the inner blanket will contract and the pressure of the contacting surfaces of core hexagonal tube and inner blanket hexagonal tube will remain balanced.

Since the same kind of hexagonal tubes are used in the core and inner blanket, the thermal expansion of the hexagonal tubes in the core will amount to a fraction $(R_4 - R_3)/R_4$ of the free expansion.

The temperature of the hexagonal tube is dependent on the temperature of coolant flowing in the channel partly formed by the hexagonal tube. This temperature is calculated from the following equations:

$$C_f s\,\theta_f(\chi,s) = \dot{Q}_g(1-\gamma) - \dot{Q}_c \quad ; \tag{7.1}$$

$$C_c s\,\theta_c(\chi,s) = \dot{Q}_c - (\dot{Q}_n - \gamma\dot{Q}_g) \quad ; \tag{7.2}$$

$$\dot{Q}_n - \gamma\dot{Q}_g = 2\pi R_2 H_2 \{\theta_c(\chi,s) - \theta_n(\chi,s)\} \quad ; \tag{7.3}$$

$$\dot{Q}_n = C_n s\theta_n(\chi,s) + vC_n \frac{d\theta_n(\chi,s)}{d\chi} + H_3\{\theta_n(\chi,s) - \theta_t(\chi,s)\} \quad ; \tag{7.4}$$

$$C_t s\ \theta_t(\chi,s) + H_3\ \{\theta_n(\chi,s) - \theta_t(\chi,s)\} \quad . \tag{7.5}$$

From Eqs. (4.12) and (7.1) through (7.5), the $\theta_t(\chi,s)$ are (see Appendix E)

$$\theta_n(\chi,s) = \{\gamma + (1-\gamma)\ \xi\ (s)\}\frac{1}{vC_n}\int_0^{\chi} \dot{Q}_g(\chi',s)\, e^{\zeta(s)(\chi'-\chi)}\, d\chi' \quad , \tag{7.6}$$

$$\theta_t(\chi,s) = \frac{\theta_n(\chi,s)}{1 + (C_t/H_3)\ s} \quad , \tag{7.7}$$

where

$$\zeta(s) = \frac{s}{vC_n}\left[C_n + \frac{C_t}{1+(C_t/H_3)\ s} + \frac{C_c + C_f F(s)}{1 + \dfrac{s}{2\pi R_2 H_2}\{C_c + C_f\ F(s)\}}\right] \quad . \tag{7.8}$$

By using a procedure similar to that in Section IV, we may calculate that the power generation rate to hexagonal tube temperature transfer function is (see Appendix F)

$$\frac{\bar{\theta}_t(s)}{\dot{Q}_g(s)} = \frac{\bar{H}_1(1+\tau_8 s)(1+\tau_3 s)(1+\tau_4 s)(1+\tau_{13} s)}{(1+\tilde{\tau}_2 s)(1+\gamma_1 s+\gamma_2 s^2+\gamma_3 s^3+\gamma_4 s^4)}$$

$$\left[- \frac{\bar{H}_2 + \bar{H}_7 s + \bar{H}_8 s^2 + \bar{H}_9 s^3}{(1+\tau_3 s)(1+\tau_4 s)(1+\tau_{13} s)} + \frac{\bar{H}_4\{1+\tau_3+\tau_4)s\}(1+\tau_{13} s)}{1+\delta_1 s+\delta_2 s^2+\delta_3 s^3} \right.$$

$$\left. + \frac{\{1+(\tau_3+\tau_4)s\}^2(1+\tau_{13} s)^2}{1+\gamma_1 s+\gamma_2 s^2+\gamma_3 s^3+\gamma_4 s^4} \quad \frac{1-\bar{H}_5+\bar{H}_{10} s+\bar{H}_{11} s^2+\bar{H}_{12} s^3}{1+\delta_1 s+\delta_2 s^2+\delta_3 s^3} \right]$$

$$+ \frac{{}_b\dot{Q}_g(s)}{\dot{Q}_g(s)} \frac{{}_b\theta_n({}_bL,s)}{{}_b\dot{Q}_g(s)} \frac{1}{1+T_r s} \frac{1}{1+\tau_{13} s} \quad . \tag{7.9}$$

The radial displacement r_2 of the core due to hexagonal tube temperature is

$$r_2 = \frac{R_4 - R_3}{R_4} \left[\frac{\Delta \ell}{\ell} / {}^\circ C \right]_{SS} R_3 \, \bar{\theta}_t(s) \quad . \tag{7.10}$$

The power generation rate to core radial displacement due to the thermal expansion transfer function is, then,

$$\frac{\bar{r}_2(s)}{\dot{Q}_g(s)} = \frac{R_3 - R_4}{R_4} \left[\frac{\Delta \ell}{\ell} / {}^\circ C \right]_{SS} R_3 \frac{\bar{\theta}_t(s)}{\dot{Q}_g(s)} \quad . \tag{7.11}$$

VIII. ESTIMATION OF THE REACTIVITY COEFFICIENT

1. Coolant Temperature Coefficient in the Core

The reactivity is reduced by the decrease in coolant density. The temperature coefficient of the coolant calculated for the EBR-I Mark III[2] was assumed to be the same for the EBR-I Mark IV. Then,

$$K_n \simeq - 1.4 \times 10^{-6} \, \Delta K/K/{}^\circ C \quad . \tag{8.1}$$

If the effect of NaK temperature in the NaK bond is considered in the temperature effect of the jacket, the effective coolant temperature coefficient will be

$$K_{nc} = K_n \frac{a_n - a_{nb}}{a_n} = K_n \frac{0.1768}{0.2387} \simeq 1.0 \times 10^{-6} \Delta K/K/{}^\circ C \quad . \tag{8.2}$$

2. Fuel Temperature Coefficient in the Core

The fuel temperature coefficient is considered as the sum of two effects: 1) the increase of core height due to axial fuel expansion may reduce the reactivity, and 2) the decrease of NaK volume in the NaK bond due to radial fuel expansion may reduce the reactivity. Effect 1) was estimated for EBR-I Mark IV from the calculations for ZPR-III to be

$$K_{f_1} \simeq - 3.01 \times 10^{-6}\ \Delta K/K/°C \quad . \tag{8.3}$$

Effect 2) can be calculated as follows:

$$K_{f_2} \simeq K_n \frac{a_f[\Delta \ell/\ell/°C]_{Pu} \times 2}{a_n[\Delta \rho/\rho/°C]_{NaK}} = K_n \frac{0.2727 \times 12.5 \times 10^{-6} \times 2}{0.2387 \times 3 \times 10^{-4}}$$

$$\simeq - 0.14 \times 10^{-6}\ \Delta K/K/°C \quad . \tag{8.4}$$

The effective fuel temperature coefficient is, therefore,

$$K_f = K_{f_1} + K_{f_2} \simeq - 3.15 \times 10^{-6}\ \Delta K/K/°C \quad . \tag{8.5}$$

3. Jacket and NaK Bond Temperature Coefficient

In the analysis, the jacket and NaK bond are considered together, so their temperature coefficient must be considered together.

The temperature coefficient of the NaK bond is

$$K_{nb} = K_n \frac{a_{nb}}{a_n} \simeq - 0.4 \times 10^{-6}\ \Delta K/K/°C \quad . \tag{8.6}$$

The reactivity effect due to the jacket temperature is similar to effect 2) of the fuel temperature, and it can be calculated as follows

$$K_{zj} = K_n \frac{a_j\,[\Delta \ell/\ell/°C]_{Zr} \times 2}{a_n[\Delta \rho/\rho/°C]_{NaK}} = K_n \frac{0.1183 \times 9.6 \times 10^{-6} \times 2}{0.2387 \times 3 \times 10^{-4}}$$

$$= - 0.045 \times 10^{-6}\ \Delta K/K/°C \quad . \tag{8.7}$$

The effective jacket temperature coefficient will be

$$K_j = K_{nb} + K_{zj} \simeq - 0.445 \times 10^{-6}\ \Delta K/K/°C \quad . \tag{8.8}$$

4. Reactivity Coefficient of the Radial Displacement of Core

The reactivity coefficient of the radial displacement of core may be given as follows:

$$K_d = \frac{\Delta K/K}{\Delta r} = 2\,K_{f_1} \frac{1}{[\Delta \ell/\ell/°C]_{Pu} \times R_c} = \frac{1}{12.5 \times 10^{-6} \times 9.037}$$

$$= -5.319 \times 10^{-2}\ \Delta K/K/\Delta r \quad . \tag{8.9}$$

5. Temperature Coefficients of Upper Blanket Coolant and Blanket Slug.

The temperature coefficients of the upper blanket coolant and blanket slug were calculated for the EBR-I Mark III,[2] and the assumption was made that they have the same values for EBR-I Mark IV. Then,

$$_uK_n = -0.2 \times 10^{-6}\ \Delta K/K/°C \tag{8.10}$$

and

$$_uK_f = -0.23 \times 10^{-6}\ \Delta K/K/°C \quad . \tag{8.11}$$

6. Check on the Experimental Results for Isothermal Reactivity Coefficient.

The isothermal reactivity coefficient was measured as $31.5 \times 10^{-6} \Delta K/K/°C$.

This coefficient includes the effects of core radial expansion, lower blanket temperature rise, and inner blanket temperature rise, but does not include the fuel-slug bowing effect.

The core radial expansion temperature coefficient is then calculated as

$$K_r = 2K_{f_1} \frac{[\Delta \ell/\ell/°C]_{SS}}{[\Delta \ell/\ell/°C]_{Pu}} = 2K_{f_1} \frac{18 \times 10^{-6}}{12.5 \times 10^{-6}}$$

$$= 8.67 \times 10^{-6}\ \Delta K/K/°C \quad . \tag{8.12}$$

The lower blanket temperature coefficient is obtained as

$$_1K_n = {}_uK_n \frac{3.552}{7.745} \simeq -0.092 \times 10^{-6}\ \Delta K/K/°C \quad ; \tag{8.13}$$

$$_1K_f = {}_uK_f \frac{3.552}{7.745} \simeq -0.105 \times 10^{-6}\ \Delta K/K/°C \quad . \tag{8.14}$$

The inner blanket temperature coefficient was calculated for the EBR I Mark III.[2] The same value was assumed for the EBR-I Mark IV. Then,

$$ {}_{b}K_{n} = -\ 2.262 \times 10^{-6}\ \Delta K/K/°C \quad ; \tag{8.15} $$

$$ {}_{b}K_{f_1} = -\ 1.793 \times 10^{-6}\ \Delta K/K/°C \quad ; \tag{8.16} $$

$$ {}_{b}K_{f_2} = K_{n} \frac{{}_{i}a_{f}[\Delta \ell/\ell/°C]_{U} \times 2}{{}_{i}a_{n}[\Delta \rho/\rho/°C]_{NaK}} = {}_{b}K_{n} \frac{0.6714 \times 14 \times 10^{-6} \times 2}{0.2632 \times 3 \times 10^{-4}} $$

$$ = -\ 0.539\ \Delta K/K/°C \quad . \tag{8.17} $$

The blanket radial expansion temperature coefficient is

$$ {}_{u}K_{r} = 2_{u}K_{f} \frac{[\Delta \ell/\ell/°C]_{SS}}{[\Delta \ell/\ell/°C]_{U}} = 2_{u}K_{f} \frac{18 \times 10^{-6}}{14 \times 10^{-6}} = -\ 0.593 \times 10^{-6}\ \Delta K/K/°C \quad ; \tag{8.18} $$

$$ {}_{1}K_{r} = 2_{1}K_{f} \frac{[\Delta \ell/\ell/°C]_{SS}}{[\Delta \ell/\ell/°C]_{U}} = 2_{1}K_{f} \frac{18 \times 10^{-6}}{14 \times 10^{-6}} = -\ 0.264 \times 10^{-6}\ \Delta K/K/°C \quad ; \tag{8.19} $$

$$ {}_{b}K_{r} = 2_{b}K_{f} \frac{[\Delta \ell/\ell/°C]_{SS}}{[\Delta \ell/\ell/°C]_{U}} = 2_{b}K_{f} \frac{18 \times 10^{-6}}{14 \times 10^{-6}} = -\ 4.609 \times 10^{-6}\ \Delta K/K/°C, \tag{8.20} $$

and the isothermal temperature coefficient is

$$ K_{it} = K_{nc} + K_{f} + K_{j} + {}_{u}K_{n} + {}_{u}K_{f} + K_{r} + {}_{1}K_{n} + {}_{1}K_{f} + {}_{i}K_{n} $$

$$ + {}_{b}K_{f_1} + {}_{b}K_{f_2} + {}_{u}K_{r} + {}_{1}K_{r} + {}_{i}K_{r} $$

$$ = -23.952 \times 10^{-6}\ \Delta K/K/°C \quad . \tag{8.21} $$

Since the calculated values are not too different from the experimental value, the calculated values are used in the analysis.

IX. BLOCK DIAGRAM OF EBR-I MARK IV TRANSFER FUNCTION

The block diagram of the transfer function is shown in Fig. 9.1. The transfer function for each block listed in Table 9.1.

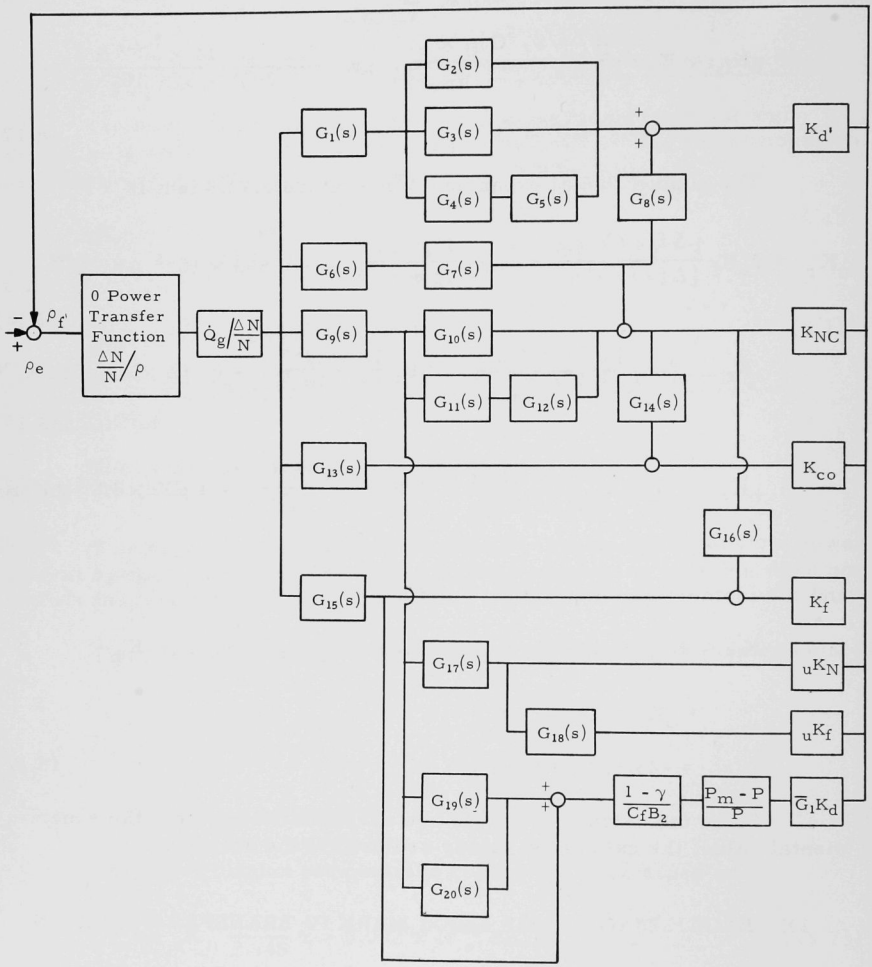

Fig. 9.1. Block Diagram of the Transfer Function

Table 9.1

TRANSFER FUNCTIONS INDICATED IN FIG. 9.1

$$G_1(s) = \frac{\overline{H}_1(1+\tau_8 s)(1+\tau_3 s)(1+\tau_4 s)(1+\tau_{13} s)}{(1+\tilde{\tau}_2 s)(1+\gamma_1 s+\gamma_2 s^2+\gamma_3 s^3+\gamma_4 s^4)}$$

$$G_2(s) = \frac{-\overline{H}_2+\overline{H}_7 s+\overline{H}_8 s^2+\overline{H}_9 s^3}{(1+\tau_3 s)(1+\tau_4 s)(1+\tau_{13} s)}$$

$$G_3(s) = \frac{\overline{H}_4\{1+(\tau_3+\tau_4)s\}(1+\tau_{13} s)}{1+\delta_1 s+\delta_2 s^2+\delta_3 s^3}$$

$$G_4(s) = \frac{\{1+(\tau_3+\tau_4)s^2(1+\tau_{13} s)^2}{1+\gamma_1 s+\gamma_2 s^2+\gamma_3 s^3+\gamma_4 s^4}$$

$$G_5(s) = \frac{1-\overline{H}_5+\overline{H}_{10} s+\overline{H}_{11} s^2+\overline{H}_{12} s^3}{1+\delta_1 s+\delta_2 s^2+\delta_3 s^3}$$

$$G_6(s) = \frac{({}_b\dot{Q}_g/\dot{Q}_g)({}_bL/{}_bC_{n\ b^v})(1+{}_b\tau_8 s)}{\{(1+{}_b\tau_3 s)(1+{}_b\tau_4 s)+{}_b\tau_{0/2}s(1+{}_b\tau_6 s)(1+{}_b\tau_7 s)\}}$$

$$G_7(s) = \frac{1}{(1+{}_b\tilde{\tau}_2 s)(1+T_r s)}$$

$$G_8(s) = \frac{1}{1+\tau_{13} s}$$

$$G_9(s) = \frac{(1+\tau_8 s)}{(1+\tilde{\tau}_2 s)(1+\alpha_1 s+\alpha_2 s^2+\alpha_3 s^3)}$$

$$G_{10}(s) = \overline{A}_1(\overline{C}_1+\overline{C}_2 s+\overline{C}_3 s^2)$$

$$G_{11}(s) = \frac{(1+\tau_3 s)(1+\tau_4 s)}{(1+\beta_1 s+\beta_2 s^2)}$$

$$G_{12}(s) = \frac{\overline{C}_4+\overline{C}_5 s+\overline{C}_6 s^2+\overline{C}_7 s^3+\overline{C}_8 s^4}{1+\alpha_1 s+\alpha_2 s^2+\alpha_3 s^3}$$

$$G_{13}(s) = \frac{\overline{B}_1(1+\tau_5 s)}{(1+\tilde{\tau}_2 s)(1+\tau_3 s)(1+\tau_4 s)}$$

$$G_{14}(s) = \frac{(1+\tau_1 s)}{(1+\tau_3 s)(1+\tau_4 s)}$$

Table 9.1. (Contd.)

$$G_{15}(s) = \frac{\overline{B}_2\,(\overline{B}_3 + \overline{B}_4 s + \overline{B}_5 s^2)}{(1 + \tilde{\tau}_2 s)(1 + \tau_3 s)(1 + \tau_4 s)}$$

$$G_{16}(s) = \frac{1}{(1 + \tau_3 s)(1 + \tau_4 s)}$$

$$G_{17}(s) = \frac{A}{v\,C_n B} \cdot \frac{\overline{D}_6 + \overline{D}_7 s + \overline{D}_8 s^2 + \overline{D}_9 s^3 + \overline{D}_{10} s^4}{(1 + \overline{E}_1 s + \overline{E}_2 s^2)(1 + \beta_1 s + \beta_2 s^2)}$$

$$G_{18}(s) = (1 + \tau_{12} s)$$

$$G_{19}(s) = \frac{\{C_f\,\overline{B}_2/(1 - \gamma)\}(1/v\,C_n B)(1 + \tau_5 s)(F_2 + F_4 s + F_5 s^2)}{(1 + \tilde{\tau}_2 s)(1 + \tau_3 s)(1 + \tau_4 s)}$$

$$G_{20}(s) = \frac{\{C_f\,\overline{B}_2/(1 - \gamma)\}(1/v\,C_n B)(1 + \tau_5 s)F_3\{1 + (\tau_3 + \tau_4)s + \tau_3 \tau_4 s^2\}}{(1 + \tilde{\tau}_2 s)(1 + \beta_1 s + \beta_2 s^2)}$$

X. DISCUSSION OF THE ANALYSIS

The analytical results for several flow rates at 1200-kw operation are shown in Fig. 10.1. The experimental results for a flow rate of 280 gpm and a power level of 1200 kw are given in Fig. 10.2.

An inspection of Fig. 10.1 and 10.2 reveals that the analytical results are characterized by a sharp resonance which contrasts with the broader resonance noted experimentally. This sharp resonance is considered as follows:

(1) In Appendix F, the approximation of the term $\frac{1}{1 + \{\zeta(s)/B\}^2}$ in Eq. (F.1) is sufficiently exact. The approximation of the term $e^{-\zeta(s)L}$ in the equation, however, is insufficiently exact. In practice, when the denominator of Eq. (F.1) goes to zero at some frequency, the numerator also goes to zero and the limiting value of this equation is finite at that frequency. In the approximate equation, Eq. (F.7), however, this relation is not satisfied and the frequency at which the denominator goes to zero is not the same as that at which the numerator goes to zero.

(2) In the approximate equations (B.16), (C.1), and (D.1), the same problems as discussed in (1) also appear.

If the following equations are used instead of the Eqs. (B.16), (C.1), (D.1), and (F.7), such problems may be avoided.

$$\frac{\overline{\theta}_n(s)}{\dot{Q}_g(s)} \simeq \frac{1 + \tau_8 s}{(1+\tilde{\tau}_2 s)(1+\tau_6 s)(1+\tau_7 s)} \frac{\overline{A}_1\overline{A}_0}{1+\tau_\alpha s} + \frac{{}_b\dot{Q}_g(s)}{\dot{Q}_g(s)} \frac{{}_b\theta_n(L,s)}{{}_b\dot{Q}_g(s)} \frac{1}{1+T_r s} \quad ; \tag{10.1}$$

$$\frac{\theta_n(Ls)}{\dot{Q}_f(s)} \simeq \frac{(1+\tau_8 s)}{(1+\tilde{\tau}_2 s)(1+\tau_6 s)(1+\tau_7 s)} \frac{\overline{D}_6 A/(vC_nB)}{1+\tau_6 s} \quad ; \tag{10.2}$$

$$\dot{Q}_f(s) \simeq \frac{(1-\gamma)\dot{Q}_g(s)}{C_f} \frac{\overline{B}_3 + \overline{B}_4 s + \overline{B}_5 s^2}{(1+\tilde{\tau}_2 s)(1+\tau_3 s)(1+\tau_4 s)}$$

$$+ \frac{\dot{Q}_g(s)(1+\tau_5 s)(1+\tau_8 s)}{(1+\tilde{\tau}_2 s)^2(1+\tau_3 s)(1+\tau_4 s)(1+\tau_6 s)(1+\tau_7 s)} \frac{(\overline{F}_2+\overline{F}_3)/vC_nB}{(1+\tau_\gamma s)} \quad ; \tag{10.3}$$

$$\frac{\overline{\theta}_t(s)}{\dot{Q}_g(s)} \simeq \frac{\overline{H}_1(1+\tau_8 s)}{(1+\tilde{\tau}_2 s)(1+h_1 s+h_2 s^2+h_3 s^3)} \frac{\overline{H}_0}{1+\tau_{16} s} + \frac{{}_b\dot{Q}_g(s)}{\dot{Q}_g(s)}$$

$$\cdot \frac{{}_b\theta_n(L,s)}{{}_b\dot{Q}_g(s)} \frac{1}{1+T_\gamma s} \frac{1}{1+\tau_{13} s} \quad , \tag{10.4}$$

where

$$\overline{A}_0 = -\overline{A}_2 + \overline{A}_4 - \overline{A}_5 + 1 \quad ;$$

$$\tau_\alpha = (-\overline{A}_2 + \overline{A}_4 - \overline{A}_5 + 1)\, \tau_{10}^2/\overline{A}_3 \quad ;$$

$$\tau_\beta = \frac{\tau_{10}^2 (\overline{D}_4 + \overline{D}_5)}{\overline{D}_1\overline{D}_2} \quad ;$$

$$\tau_\gamma = \frac{(\overline{F}_2 + \overline{F}_3)\tau_{10}}{\overline{F}_1} \quad ;$$

$$H_0 = -\overline{H}_2 + \overline{H}_4 - \overline{H}_5 + 1 \quad ;$$

$$\tau_{16} = (\overline{H}_0 \tau_{14}^2)/\overline{H}_3 \quad .$$

The analytical results obtained are shown in Fig. 10.3 and 10.4. Figure 10.5 gives the analytical results when the hexagonal-tube expansion effect is neglected. A comparison of Fig. 10.4 and 10.5 reveals that the smaller resonance originates as the result of hexagonal-tube expansion.

The data of Fig. 10.3 demonstrate that the most sensitive factor affecting the transfer function is reactor power. According to Fig. 10.2 and 10.4, the analytical and experimental results for the resonance frequency and for the sharpness of the transfer function amplitude at the resonance frequency differ.

The reasons for these differences are:

(a) As discussed in Section VIII, the theoretically derived values of the temperature coefficients used in the analysis are smaller than those measured experimentally. In addition, in estimating the isothermal temperature coefficient (see Section VIII), the calculated component of the core radial expansion was based on free expansion although in practice the outer periphery of the inner blanket was constrained. This means that theoretically derived temperature coefficients are smaller than those measured experimentally. For this reason the gain at low frequencies for the analytical treatment is larger than that determined experimentally.

(b) Since Eqs. (10.1) through (10.4) are simple approximations, resonance effects will be restrained.

(c) In the analytical treatment it was assumed that fuel-rod displacement is dictated by hexagonal-tube expansion. Thus, it is reasonable to assume a like time delay for hexagonal-tube expansion and fuel-rod displacement. In addition, if the hexagonal-tube expansion is not equal axially, then the relationship between the hexagonal-tube expansion and fuel-rod displacement becomes a very complicated phenomenon because of the elasticity and rigidity of the fuel rods. Accordingly, the time delay mentioned above will not be approximated by a simple first-order transfer function. If this time-delay effect is applied to the analysis, the resonance frequency would tend to decrease and would be closer to that of the experimental result.

(d) Since the tightening action of the core clamps may not be uniform axially and the hexagonal tubes of the inner blanket conceivably could bend, this possibility suggests that the expansion of the hexagonal tube may be larger than that given by the analytical value. Under these circumstances, the hexagonal-tube expansion effects would then be more significant than those given by the analytical treatment and would tend to decrease the gain at low frequencies for the same reason as in (a).

For example, if the time delay for radial expansion of the core is assumed, it is to be as follows:

$$\frac{\text{displacement of fuel rod}}{\text{displacement of hexagonal tube}} = \frac{1}{(1+\tau s)^2} \quad , \tag{10.5}$$

where

$$\tau \simeq \sqrt{\sqrt{2}-1} \quad ,$$

and the reactivity coefficient due to radial expansion of the core is assumed to equal successively: (1) the calculated value, (2) two times the calculated

value, and (3) three times the calculated value; the analytical results are shown in Fig. 10.6. As can be seen, when the reactivity coefficient is assumed to be three times the calculated value, the calculated transfer function shows very close agreement with that obtained by experiment. This would also indicate that the above discussion is reasonable.

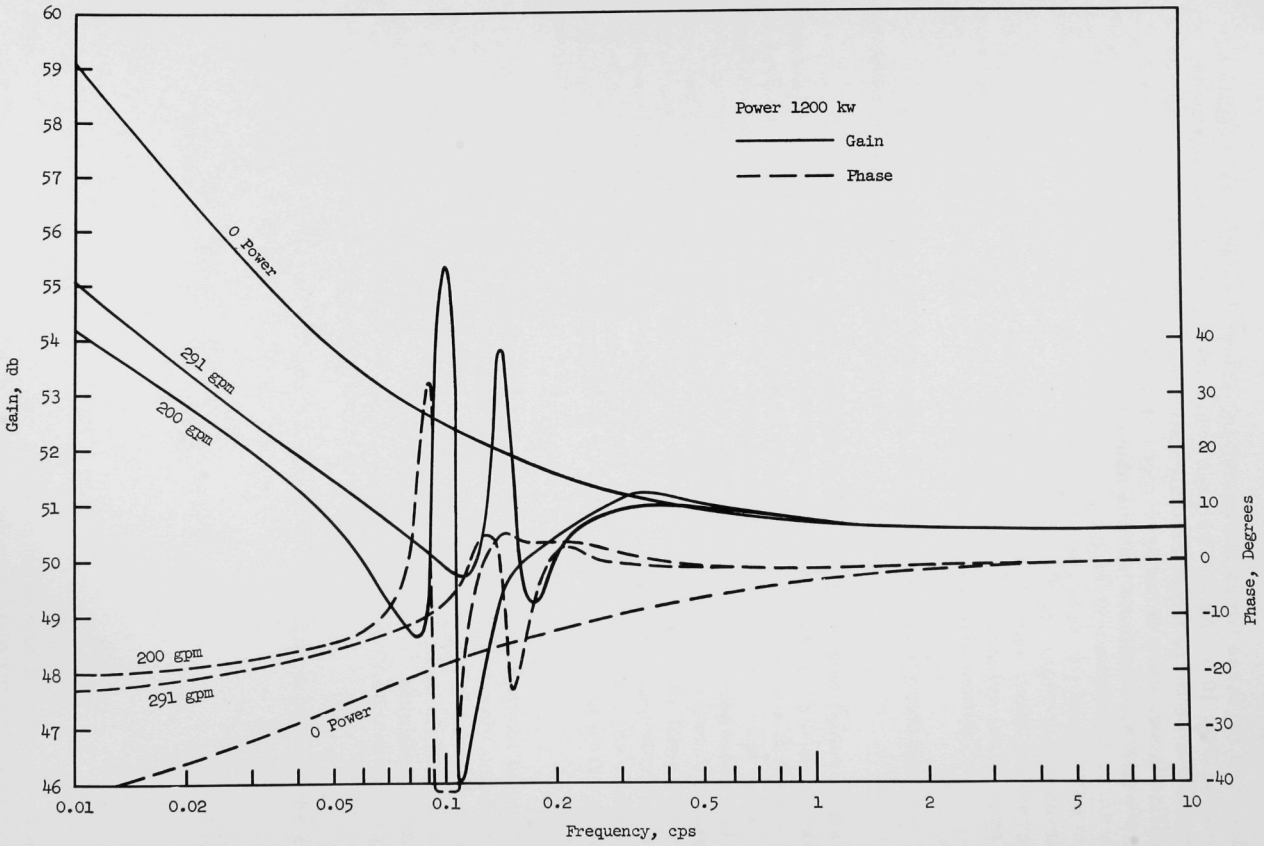

Fig. 10.1. Analytical Results for EBR-I Mark IV Transfer Functions for 1200 kw

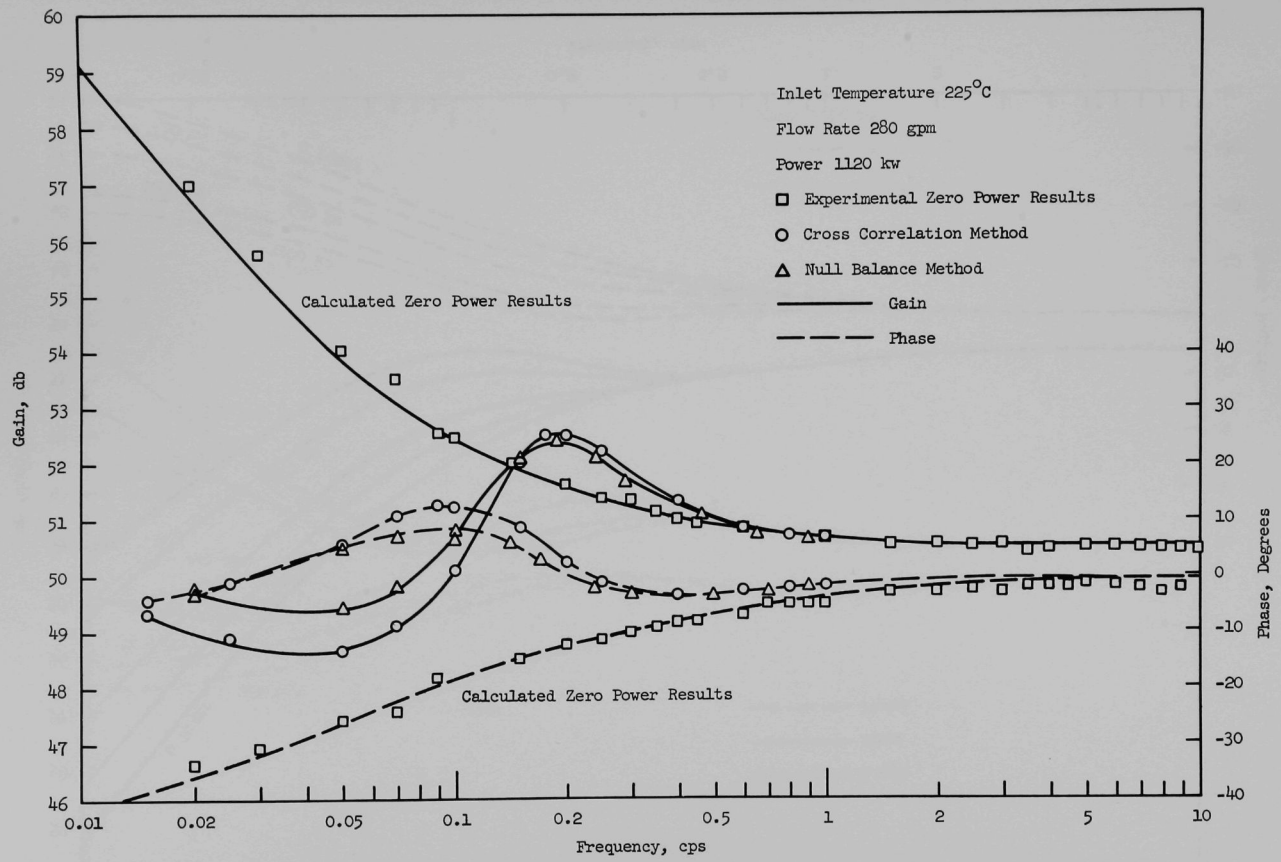

Fig. 10.2. EBR-I, Mark IV Transfer Function

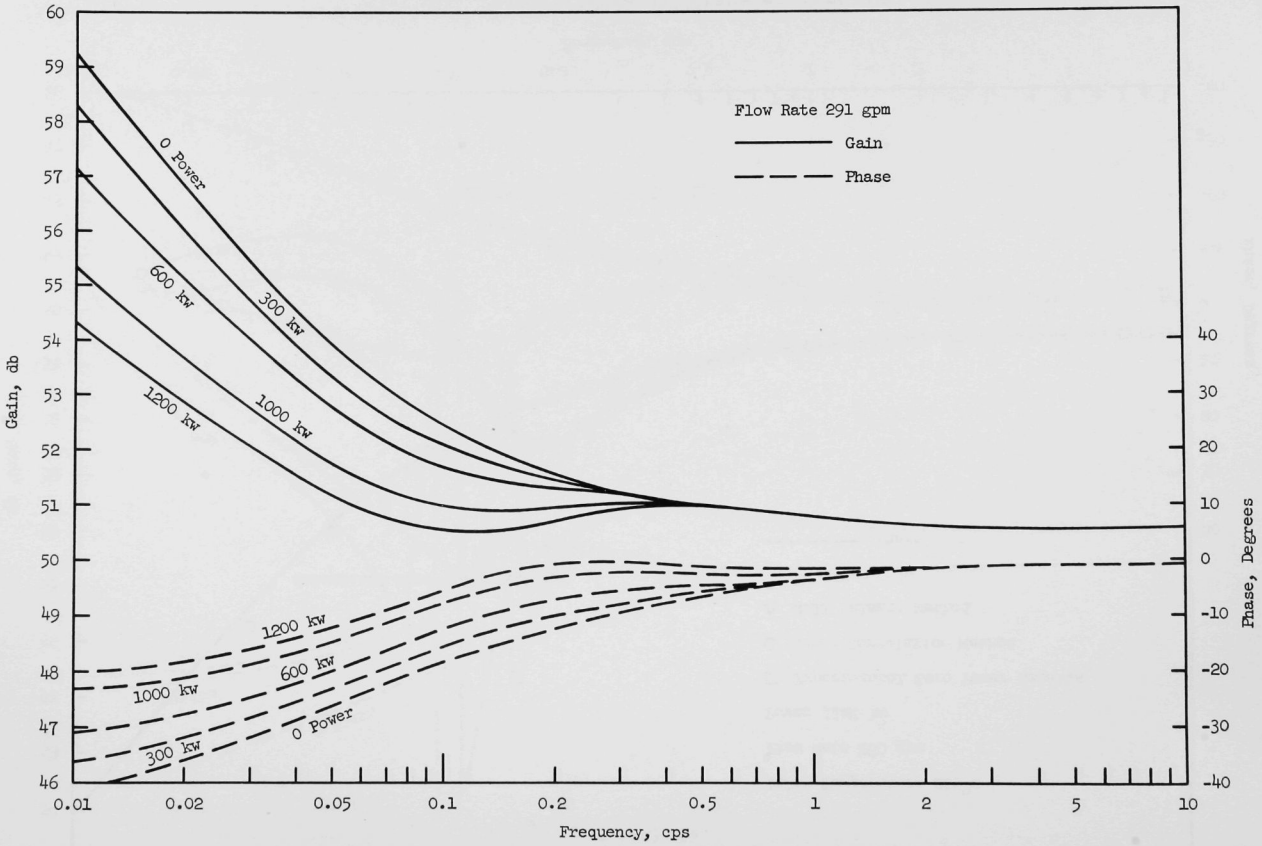

Fig. 10.3. Analytical Results for EBR-I Mark IV Transfer Function at a Flow Rate of 291 gpm

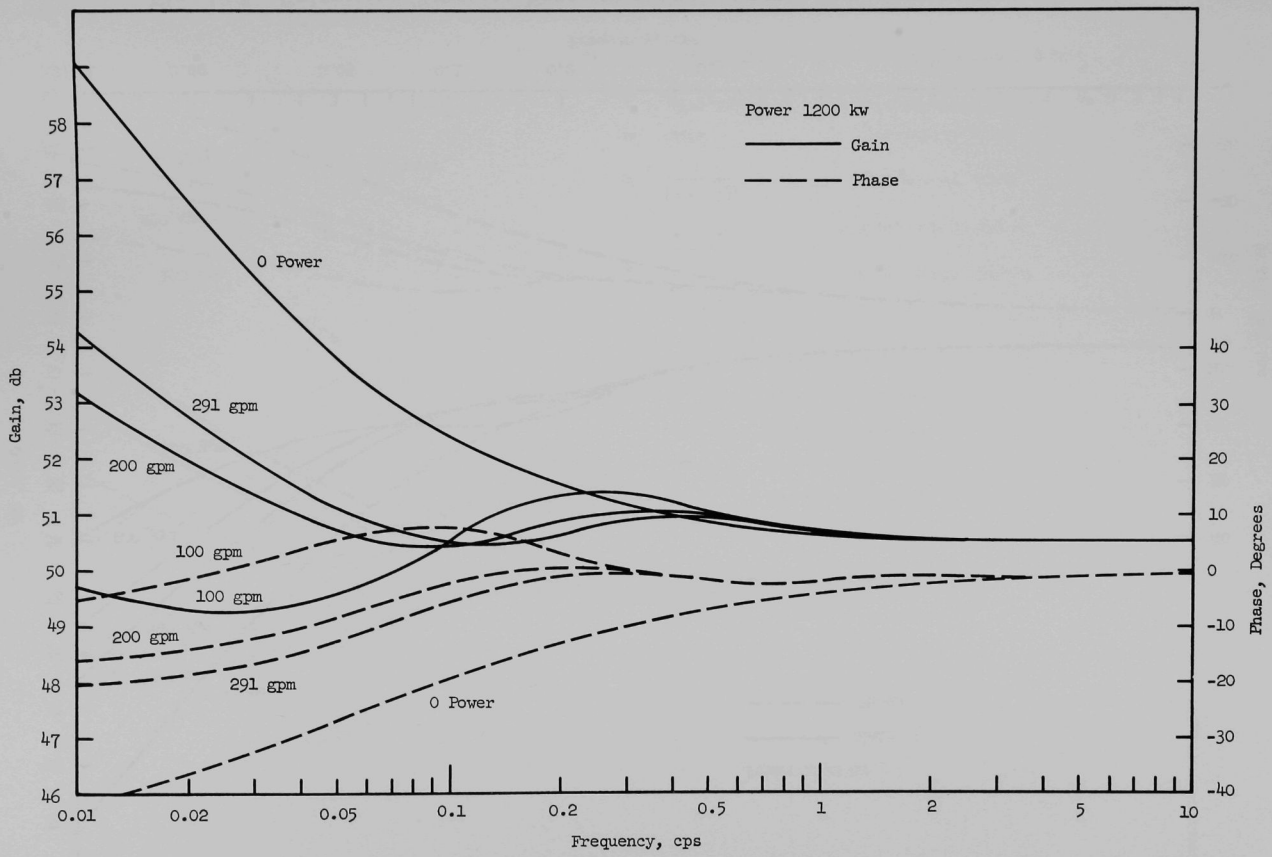

Fig. 10.4. Further Analytical Results for EBR-I Mark IV Transfer Functions at 1200 kw

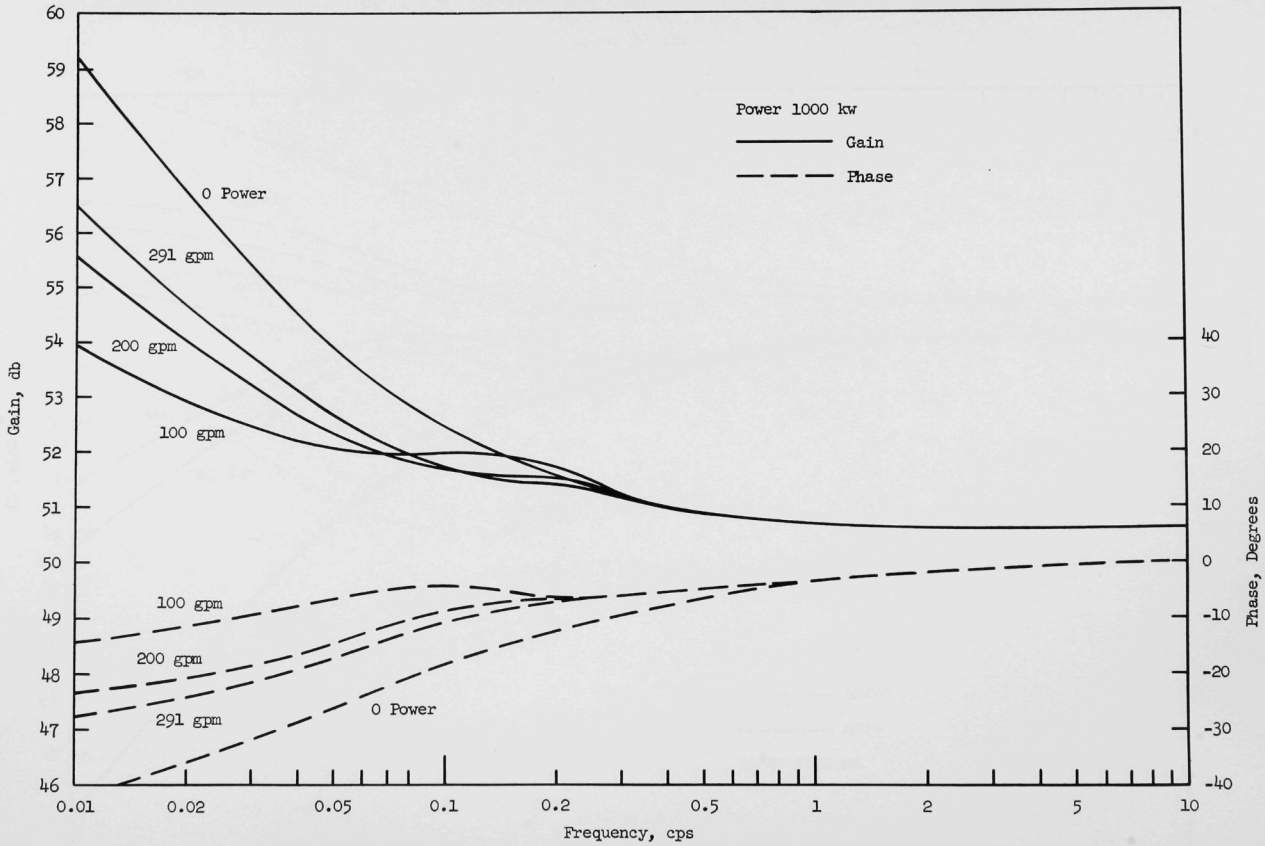

Fig. 10.5. Calculated Transfer Function with Hexagonal Tube Expansion Neglected

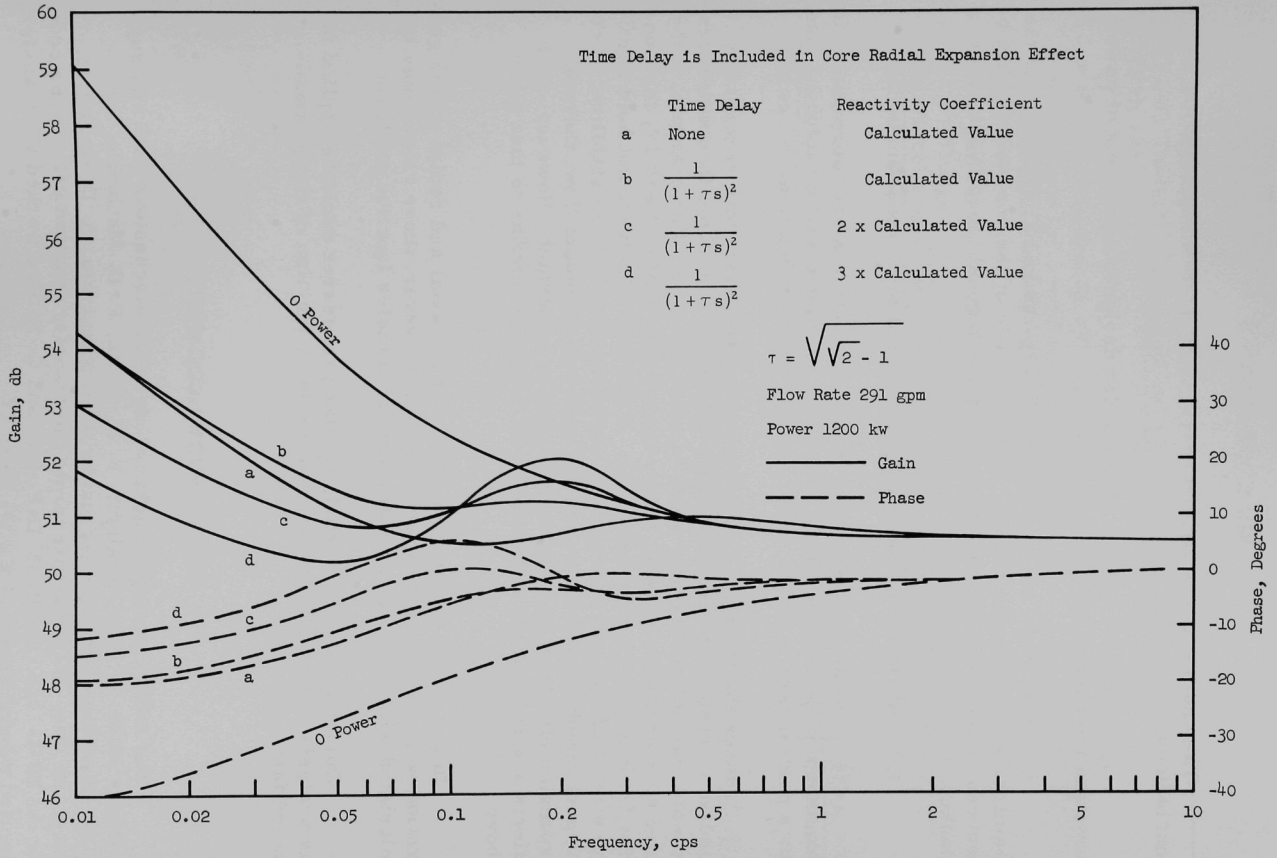

Fig. 10.6. Analytical Results for EBR-I Mark IV Transfer Function with Inclusion of Time Delay in Radial Expansion of the Core

XI. CONCLUSIONS

The analytical results discussed above permit the following conclusions:

(1) EBR-I Mark IV is stable under designed conditions of power, flow, and inlet temperature.

(2) The small resonance is caused by the radial expansion of the stainless steel hexagonal tubes. The magnitude of the resonance could be reduced by increasing the thickness of the hexagonal tubes in the inner blanket.

(3) Decreases in coolant flow rate tend to increase instability.

(4) The approximate expressions of Section X are more convenient than those of Eqs. (B.16), (C.1), (D.1), and (F.7), and are sufficiently exact for a preliminary estimate of the reactor transfer function.

Since the analytical treatment presented above was specifically applied to results obtained with EBR-I Mark IV, the same feedback mechanisms may not necessarily apply to other systems. For example, if the core size were considerably larger than that of EBR-I Mark IV, the Doppler feedback may not be negligible. If the fuel rods were not held tightly, the effects of fuel-rod bowing may significantly affect the stability. If core support members are located in the core outlet coolant flow, thermal-expansion effects in these members may be important. However, such effects are susceptible to treatment in a manner similar to that given above.

In the actual evaluations, values of the axial and radial power generation were determined experimentally. However, these values may be calculated with an accuracy sufficient for transfer function analysis.

During the design period, similar procedures could be applied to the analysis of spatially independent transfer function of liquid metal-cooled fast reactors.

XII. ACKNOWLEDGMENTS

The author gratefully acknowledges the discussions with and suggestions made by F. W. Thalgott, R. R. Smith, F. D. McGinnis, and R. O. Haroldsen. My special thanks to H. Nakamura, R D. DeForest, and C. B. Doe. H. Nakamura wrote the transfer function calculating code for the IBM-1620, and R. D. DeForest and C. D. Doe worked the transfer function measurement of EBR-I Mark IV.

REFERENCES

1. R. O. Haroldsen, R. D. McGinnis, M. Novick, R. R. Smith, and F. W. Thalgott, Safety Analysis Report EBR-I Mark IV, ANL-6411 (Feb 1963).

2. A Fenstermacker, D. Okrent, and H. Sandmeier, Power Coefficient Calculations for EBR-I Mark III, Internal memorandum, Argonne National Laboratory (1957).

3. R. R. Smith, R. G. Matlock, F. D. McGinnis, M. Novick and F. W. Thalgott, An Analysis of the Stability of EBR-I Mark I to III and Conclusions Pertinent to the Design of Fast Reactors, International Atomic Energy Agency, Vienna (1962).

4. S. Hayashi, J. Wakabayashi, and T. Hashino, Analysis of the Transfer Function of EBR-I Mark II, National Nuclear Congress, Tokyo, Japan (Feb 1962).

5. T. Hoshino, Frequency Response of the EBR-I Mark II and Mark III, Thesis, M. S. degree, Kyoto University (March 1962).

APPENDIX A

From Eqs. (4.12) through (4.16) the following equations are obtained:

$$\dot{Q}_n(\chi,s) - \gamma\dot{Q}_g(\chi,s) = \frac{F(s)(1-\gamma)\dot{Q}_g(\chi,s) - s\{C_c + C_fF(s)\}\theta_n(\chi,s)}{1 + s\{C_c + C_fF(s)\}/2\pi R_2H_2} \quad ; \quad (A.1)$$

$$\theta_c(\chi,s) = \frac{\{\dot{Q}_n(\chi,s) - \gamma\dot{Q}_g(\chi,s)\}}{2\pi R_2H_2} + \theta_n(\chi,s) \quad ; \quad (A.2)$$

$$\theta_f(\chi,s) = \frac{(1-\gamma)\dot{Q}_g(\chi,s) - \{\dot{Q}_n(\chi,s) - \gamma\dot{Q}_g(\chi,s)\} - sC_c\ \theta_c(\chi,s)}{C_fs} \quad ; \quad (A.3)$$

$$\frac{d\theta_n(\chi,s)}{d\chi} + \theta_n(\chi,s)\frac{s}{v}\left[1 + \frac{\{C_c + C_fF(s)\}/C_n}{1 + \frac{s}{2\pi R_2H_2}\{C_c + C_fF(s)\}}\right]$$

$$= \frac{\gamma\dot{Q}_g(\chi,s)}{vC_n} + \frac{(1-\gamma)\ \dot{Q}_g(\chi,s)\ F(s)/(vC_n)}{1 + \frac{s}{2\pi R_2H_2}\{C_c + C_fF(s)\}} \quad . \quad (A.4)$$

Solving Eq. (A.4), $\theta_n(\chi,s)$ is given by

$$\theta_n(\chi,s) = \{\gamma + (1-\gamma)\xi(s)\}\frac{1}{vC_n}\int_0^{\chi}\dot{Q}_g(\chi',s)\ e^{\eta(s)(\chi'-\chi)}\,d\chi' \quad . \quad (A.5)$$

APPENDIX B

From the assumptions 5 and 3 listed in Sect. II, the power generation rate in the fuel rods in the core is radially independent, and the effective average core temperatures are denoted by the equations

$$\overline{\theta}_n(s) = \frac{1}{L}\int_0^L D(\chi)\ \theta_n(\chi,s)\, d\chi$$

$$= \frac{\{\gamma + (1-\gamma)\xi(s)\}\,\dot{Q}_g(s)\,A^2}{{}_vC_n\,B^2L}\ \frac{1}{1+\left\{\frac{\eta(s)}{B}\right\}^2}$$

$$\left[\frac{\eta(s)L}{2} - \frac{\eta(s)\{\sin 2(BL+C) - \sin 2C\}}{4B}\right.$$

$$- \frac{\sin^2(BL+C) + \sin^2 C}{2} + e^{-\eta(s)L}\sin(BL+C)\sin C$$

$$\left. + \frac{1 - e^{-\eta(s)L}\left\{\cos BL + \frac{\eta(s)}{B}\sin BL\right\}}{1+\left\{\frac{\eta(s)}{B}\right\}^2}\right]$$

$$+ {}_b\theta_{n\,b}L(s)\,e^{-T_r s}\,\frac{A}{BL}\{\cos c - \cos(BL+C)\} \quad ; \qquad (B.1)$$

$$\overline{\theta}_c(s) = \frac{1}{L}\int_0^L D(\chi)\ \theta_c(\chi,s)\, d\chi$$

$$= \frac{(1-\gamma)\xi(s)\,\dot{Q}_g(s)A^2}{2\pi R_2 H_2}\left\{\frac{1}{2} - \frac{\sin 2(BL+C) - \sin 2C}{4BL}\right\}$$

$$+ \frac{\overline{\theta}_n(s)}{1 + \frac{s}{2\pi R_2 H_2}\{C_c + C_f F(s)\}} \quad ; \qquad (B.2)$$

$$\bar{\theta}_f(s) = \frac{1}{L}\int_0^L D(\chi)\,\theta_f(\chi,s)\,d\chi$$

$$= (1-\gamma)\dot{Q}_g(s)A^2\left\{\frac{1}{C_f s} - \xi(s)\left(\frac{1}{C_f s} + \frac{C_c}{2\pi R_2 H_2 C_f}\right)\right\}$$

$$\times\left\{\frac{1}{2} - \frac{\sin 2(BL+C) - \sin 2C}{4BL}\right\} + \frac{F(s)\,\bar{\theta}_n(s)}{1 + \frac{s}{2\pi R_2 H_2}\{C_c + C_f F(s)\}} \quad ; \tag{B.3}$$

$$e^{-f(s)} \simeq \frac{1}{1+f(s)} \quad ; \tag{B.4}$$

$$\frac{1-e^{-f(s)}}{f(s)} \simeq 1 - \frac{f(s)}{2} \simeq \frac{1}{1+\frac{f(s)}{2}} \quad . \tag{B.5}$$

The power generation rate to core temperature transfer functions is obtained:

$$\frac{\bar{\theta}_n(s)}{\dot{Q}_g(s)} \simeq \bar{A}_1 \frac{1+\tau_8 s}{(1+\tilde{\tau}_2 s)(1+\tau_3 s)(1+\tau_4 s)} \frac{1}{1+\left\{\tau_{10} s \frac{(1+\tau_6 s)(1+\tau_7 s)}{(1+\tau_3 s)(1+\tau_4 s)}\right\}^2}$$

$$\times\left[-\bar{A}_2 + \bar{A}_3 s \frac{(1+\tau_6 s)(1+\tau_7 s)}{(1+\tau_3 s)(1+\tau_4 s)} + \frac{\bar{A}_4}{1+\tau_0 s \frac{(1+\tau_6 s)(1+\tau_7 s)}{(1+\tau_3 s)(1+\tau_4 s)}}\right.$$

$$\left. + \frac{1}{1+\left\{\tau_{10} s \frac{(1+\tau_6 s)(1+\tau_7 s)}{(1+\tau_3 s)(1+\tau_4 s)}\right\}^2}\left\{1 - \frac{\bar{A}_5 + \bar{A}_6 s}{1+\tau_0 s \frac{(1+\tau_6 s)(1+\tau_7 s)}{(1+\tau_3 s)(1+\tau_4 s)}}\right\}\right]$$

$$+ \frac{{}_b\dot{Q}_g(s)}{\dot{Q}_g(s)} \frac{{}_b\theta_n(L_b,s)}{{}_b\dot{Q}_g(s)} \frac{1}{1+T_r s} \quad ; \tag{B.6}$$

$$\frac{\bar{\theta}_c(s)}{\dot{Q}_g(s)} = \frac{\bar{B}_1(1+\tau_5 s)}{(1+\tilde{\tau}_2 s)(1+\tau_3 s)(1+\tau_4 s)} + \frac{(1+\tau_1 s)}{(1+\tau_3 s)(1+\tau_4 s)} \frac{\bar{\theta}_n(s)}{\dot{Q}_g(s)} \quad ; \tag{B.7}$$

$$\frac{\overline{\theta}_f(s)}{\dot{Q}_g(s)} = \overline{B}_2 \left\{ \frac{\overline{B}_3 + \overline{B}_4 s + \overline{B}_5 s^2}{(1+\tilde{\tau}_2 s)(1+\tau_3 s)(1+\tau_4 s)} \right\} + \frac{1}{(1+\tau_3 s)(1+\tau_4 s)} \frac{\overline{\theta}_n(s)}{\dot{Q}_g(s)} \quad , \qquad (B.8)$$

where

$$\frac{{}_b\theta_n({}_bL, s)}{{}_b\dot{Q}_g(s)} = \frac{(1+{}_b\tau_8 s)\,{}_bL/{}_bC_n\,{}_bv}{(1+{}_b\tilde{\tau}_2 s)(1+{}_b\tau_3 s)(1+{}_b\tau_4 s)\left\{1 + \frac{{}_b\tau_0 s}{2}\frac{(1+{}_b\tau_6 s)(1+{}_b\tau_7 s)}{(1+{}_b\tau_3 s)(1+{}_b\tau_4 s)}\right\}}$$

$$= \frac{(1+{}_b\tau_8 s)\,{}_bL/{}_bC_n\,{}_bv}{(1+{}_b\tilde{\tau}_2 s)\left\{(1+{}_b\tau_3 s)(1+{}_b\tau_4 s) + \frac{{}_b\tau_0 s}{2}(1+{}_b\tau_6 s)(1+{}_b\tau_7 s)\right\}} \qquad (B.9)$$

and

$$\tau_0 = (C_n + C_c + C_f)L/C_n v \quad ;$$

$$(1+\tau_3 s)(1+\tau_4 s) = 1 + \left(\tau_1 + \frac{C_c + C_f}{2\pi R_2 H_2}\right)s + \frac{C_c \tau_1}{2\pi R_2 H_2} s^2 \quad ;$$

$$\tau_5 = F_1 \tilde{\tau}_2 + \tilde{F}_2 \tau_1 \quad ;$$

$$(1+\tau_6 s)(1+\tau_7 s) = 1 + \frac{(C_n + C_c)2\pi R_2 H_2 \tau_1 + (C_c + C_f)C_n}{2\pi R_2 H_2 (C_n + C_c + C_f)} s + \frac{C_c C_n \tau_1 s^2}{2\pi R_2 H_2 (C_n + C_c + C_f)} \quad ;$$

$$\tau_8 = (1-\gamma)\tau_5 + \gamma\left(\tau_1 + \tilde{\tau}_2 + \frac{C_c + C_f}{2\pi R_2 H_2}\right) \quad ;$$

$$\tau_9 = C_c/(2\pi R_2 H_2) \quad ;$$

$$\tau_{10} = (C_n + C_c + C_f)/(C_n v B) = (B/L)\tau_0 \quad ;$$

$$\overline{A}_1 = A^2/v C_n L B^2 \quad ;$$

$$\overline{A}_2 = \{\sin^2(BL + C) + \sin^2 C\}/2 \quad ;$$

$$\overline{A}_3 = \frac{C_n + C_c + C_f}{C_{n^v}} \left\{ \frac{L}{2} - \frac{\sin 2(BL+C) - \sin 2C}{4B} \right\} = \tau_0 \left\{ \frac{1}{2} - \frac{\sin 2(BL+C) - \sin 2C}{BL} \right\};$$

$$\overline{A}_4 = \sin (BL+C) \sin C \quad ;$$

$$\overline{A}_5 = \cos BL \quad ;$$

$$\overline{A}_6 = \frac{C_n + C_c + C_f}{C_{n^v} B} \sin BL = \tau_{10} \sin BL \quad ;$$

$$\overline{B}_1 = \frac{(1-\gamma)A^2}{2\pi R_2 H_2} \left\{ \frac{1}{2} - \frac{\sin 2(BL+C) - \sin 2C}{BL} \right\} \quad ;$$

$$\overline{B}_2 = \frac{(1-\gamma)A^2}{C_f} \left\{ \frac{1}{2} - \frac{\sin 2(BL+C) - \sin 2C}{BL} \right\} \quad ;$$

$$\overline{B}_3 = \tau_1 F_1 + \tilde{\tau}_2 \tilde{F}_2 + \frac{C_f}{2\pi R_2 H_2} \quad ;$$

$$\overline{B}_4 = \tau_1 \tilde{\tau}_2 + \{C_c (F_1 \tau_1 + \tilde{F}_2 \tilde{\tau}_2) + C_f \tilde{\tau}_2\} / 2\pi R_2 H_2 \quad ; \quad \overline{B}_5 = \frac{C_c \tau_1 \tilde{\tau}_2}{2\pi R_2 H_2} \quad .$$

For convenience, Eq. (B.6) may be simplified by the following procedure:

$$\frac{1}{1 + \left\{ \tau_{10} s \frac{(1+\tau_6 s)(1+\tau_7 s)}{(1+\tau_3 s)(1+\tau_4 s)} \right\}^2} = \frac{(1+\tau_3 s)^2 (1+\tau_4 s)^2}{(1+\tau_3 s)^2 (1+\tau_4 s)^2 + \tau_{10}^2 s^2 (1+\tau_6 s)(1+\tau_7 s)^2}$$

$$\simeq \frac{1 + (\tau_3 + \tau_4) s^2}{1 + \alpha_1 s + \alpha_2 s^2 + \alpha_3 s^3} \quad ; \qquad \text{(B.10)}$$

$$\frac{1}{1 + \left\{ \tau_0 s \frac{(1+\tau_6 s)(1+\tau_7 s)}{(1+\tau_3 s)(1+\tau_4 s)} \right\}} \simeq \frac{1 + (\tau_3 + \tau_4) s}{1 + \beta_1 s + \beta_2 s^2} \quad . \qquad \text{(B.11)}$$

Then

$$\frac{\overline{\theta}_n(s)}{\dot{Q}_g(s)} \simeq \frac{(1+\tau_8 s)(1+\tau_3 s)(1+\tau_4 s)}{(1+\tilde{\tau}_2 s)(1+\alpha_1 s + \alpha_2 s^2 + \alpha_3 s^2)} \left[\frac{\overline{A}_1 \{\overline{C}_1 + \overline{C}_2 s + \overline{C}_3 s^2\}}{(1+\tau_3 s)(1+\tau_4 s)} \right.$$

$$\left. + \frac{\overline{A}_1 \{\overline{C}_4 + \overline{C}_5 s + \overline{C}_6 s^2 + \overline{C}_7 s^3 + \overline{C}_8 s^4\}}{(1+\beta_1 s + \beta_2 s^2)(1+\alpha_1 s + \alpha_2 s^2 + \alpha_3 s^3)} \right] + \frac{{}_b\dot{Q}_g(s)}{\dot{Q}_g(s)} \frac{{}_b\theta_n(bL, s)}{{}_b\dot{Q}_g(s)} \frac{1}{1 + T_r s} \quad ,$$

(B.12)

where

$$\bar{C}_1 = -\bar{A}_2 \quad ;$$

$$\bar{C}_2 = \bar{A}_3 - \bar{A}_2(\tau_3 + \tau_4) \quad ;$$

$$\bar{C}_3 = \bar{A}_3(\tau_6 + \tau_7) - \bar{A}_2 \tau_3 \tau_4 \quad ;$$

$$\bar{C}_4 = 1 + \bar{A}_4 - \bar{A}_5 \quad ;$$

$$\bar{C}_5 = 3(\tau_3 + \tau_4)\{1 + \bar{A}_4 - \bar{A}_5\} + \tau_0 - \bar{A}_6 \quad ;$$

$$\bar{C}_6 = 3(\tau_3 + \tau_4)^2\{1 + \bar{A}_4 - \bar{A}_5\} + (\tau_3 + \tau_4)\{2\tau_0 - 3\bar{A}_6\} + \beta_2 + \alpha_2 \bar{A}_4 \quad ;$$

$$\bar{C}_7 = (\tau_3 + \tau_4)^3\{1 + \bar{A}_4 - \bar{A}_5\} + (\tau_3 + \tau_4)^2\{\tau_0 - 3\bar{A}_6\} + (\tau_3 + \tau_4)$$
$$\{\beta_2 + (2\tau_3\tau_4 + \tau_{10}^2)\bar{A}_4\} + \alpha_3 \bar{A}_4 \quad ;$$

$$\bar{C}_8 = (\tau_3 + \tau_4)\{(\tau_3 + \tau_4)\beta_2 + \bar{A}_4\alpha_3 - (\tau_3 + \tau_4)^2 \bar{A}_6\} \quad ;$$

$$\alpha_1 = 2(\tau_3 + \tau_4) \quad ;$$

$$\alpha_2 = (\tau_3 + \tau_4)^2 + 2\tau_3\tau_4 + \tau_{10}^2 \quad ;$$

$$\alpha_3 = 2\tau_3\tau_4(\tau_3 + \tau_{10}) + 2\tau_{10}^2(\tau_6 + \tau_7) \quad ;$$

$$\beta_1 = \tau_3 + \tau_4 + \tau_0 \quad ;$$

$$\beta_2 = \tau_3 + \tau_4 + \tau_0(\tau_6 + \tau_7) \quad .$$

APPENDIX C

From Eq. (5.7) and Appendix B, the power generation rate to core outlet temperature transfer function is denoted by the following:

$$\chi_m < L;\ r_1(\chi)_{max} = \frac{\alpha\theta_{df}L^2}{2d}\left[\left(\frac{\alpha\theta_{df} - {}_u\alpha_u\theta_{df}}{\alpha\theta_{df}}\right)\left\{1 - \frac{L}{2\,(L + {}_uL)}\right\} + \frac{{}_u\alpha_u\theta_{df}(L + {}_uL)}{2\alpha\theta_{df}L}\right]^2$$

$$\leq 0.0285 \quad ;$$

$$\chi_m > L;\ r_1(\chi)_{max} = \frac{\alpha\theta_{df}L^2}{2d}\left[2\left(\frac{\alpha\theta_{df} - {}_u\alpha_u\theta_{df}}{\alpha\theta_{df}}\right)\left\{1 - \frac{L}{2(L - {}_uL)}\right\} + \frac{{}_u\alpha_u\theta_{df}(L + {}_uL)}{\alpha\theta_{df}L} - 1\right]$$

$$\leq 0.0285 \quad . \qquad \text{(C.1)}$$

where

$$\bar{D}_1 = \frac{C_f + C_c + C_n}{BC_nv} = \tau_{10} \quad ;$$

$$\bar{D}_2 = \sin(BL + C) \quad ;$$

$$\bar{D}_3 = -\sin C \quad ;$$

$$\bar{D}_4 = -\cos(BL + C) \quad ;$$

$$\bar{D}_5 = \cos C \quad ;$$

$$\bar{D}_6 = \bar{D}_4 + \bar{D}_5 \quad ;$$

$$\bar{D}_7 = \bar{D}_1(\bar{D}_2 + \bar{D}_3) + 2(\bar{D}_4 + \bar{D}_5)(\tau_3 + \tau_4) + \bar{D}_4\tau_0 \quad ;$$

$$\bar{D}_8 = \bar{D}_1\{(\bar{D}_2 + \bar{D}_3)(\tau_3 + \tau_4 + \tau_6 + \tau_7) + \bar{D}_2\tau_0\} + (\bar{D}_4 + \bar{D}_5)\{(\tau_3 + \tau_4)^2 + \tau_3\tau_4\}$$
$$+ \bar{D}_4\{\tau_0(\tau_3 + \tau_4) + \beta_2\} \quad ;$$

$$\bar{D}_9 = \bar{D}_1[(\bar{D}_2 + \bar{D}_3)\{(\tau_3 + \tau_4)(\tau_6 + \tau_7) + \tau_6\tau_7\} + \bar{D}_2\{\tau_0(\tau_6 + \tau_7) + \beta_2\}]$$
$$+ (\bar{D}_4 + \bar{D}_5)(\tau_3 + \tau_4)\tau_3\tau_4 + \bar{D}_4\{\tau_0\tau_3 + \beta_2(\tau_3 + \tau_4)\} \quad ;$$

$$\bar{D}_{10} = \bar{D}_1[(\bar{D}_2 + \bar{D}_3)(\tau_3 + \tau_4)\tau_6\tau_7 + \bar{D}_2\{\tau_0\tau_6\tau_7 + \beta_2(\tau_6 + \tau_7)\}] + \bar{D}_4\beta_2\tau_3\tau_4$$

and

T'_r = the coolant transport time from the inner blanket outlet to the core outlet.

By substituting Eqs. (5.6) and (C.1) into the Eqs. (5.8) through (5.10), the following transfer functions result:

$$\frac{{}_u\bar{\theta}_f(s)}{\dot{Q}_g(s)} = \frac{1}{1 + \tau_{12}s} \frac{{}_u\bar{\theta}_n(s)}{\dot{Q}_g(s)} \quad ; \tag{C.2}$$

$$\frac{{}_u\bar{\theta}_n(s)}{\dot{Q}_g(s)} = \frac{\theta_n(L,s)}{\dot{Q}_g(s)} \frac{1 + \tau_{12}s}{1 + \bar{E}_1 s + \bar{E}_2 s^2} \quad , \tag{C.3}$$

where

$$\bar{E}_1 = \tau_{12} + \frac{2\pi R_2\, {}_uH_2\, {}_uL}{2\, {}_uC_n\, {}_uv}(\tau_{11} + \tau_{12}) = \tau_{12} + \frac{{}_uL}{2v} + \frac{{}_uL}{2v}\frac{\tau_{12}}{\tau_{11}} \quad ;$$

$$\bar{E}_2 = \frac{2\pi {}_uR_2\, {}_uH_2\, {}_uL}{2\, {}_uC_n v}\, \tau_{11}\, \tau_{12} = \frac{{}_uL}{2v}\, \tau_{12} \quad ;$$

$$\tau_{11} = {}_uC_n / 2\pi R_2\, {}_uH_2 \quad ;$$

$$\tau_{12} = {}_uC_f / 2\pi R_2\, {}_uH_2 \quad .$$

APPENDIX D

Since the core inlet coolant temperature is independent of the core radial position, the coolant preheating in the inner blanket does not affect the fuel-slug bowing. From Eqs. (4.17) and (4.19), the average fuel slug temperature is obtained:

$$\bar{\theta}_f'(s) = \frac{1}{L}\int_0^L \theta_f(\chi, s)\, d\chi$$

$$= \dot{Q}_g(s)\left[(1-\gamma)\left\{\frac{1}{C_f s} - \xi(s)\left(\frac{1}{C_f s} + \frac{C_c}{2\pi R_2 H_2 C_f}\right)\right\}\right.$$

$$+ \{\gamma + (1-\gamma)\xi(s)\}\frac{\xi(s)}{vC_n B}\,\frac{1}{1+\left(\frac{\eta(s)}{B}\right)^2}\left\{\frac{\eta(s)}{B} + \frac{A}{L\eta(s)}\cos C\right.$$

$$\left.\left. - \frac{A}{BL}\sin(BL+C) + e^{-\eta(s)L}\left(\frac{A}{LB}\sin C - \frac{A}{L\eta(s)}\cos C\right)\right\}\right]$$

$$\simeq \dot{Q}_g(s)\left[\frac{(1-\gamma)}{C_f}\left\{\frac{\bar{B}_3 + \bar{B}_4 s + \bar{B}_5 s^2}{(1+\tilde{\tau}_2 s)(1+\tau_3 s)(1+\tau_4 s)}\right\}\right.$$

$$+ \frac{(1+\tau_8 s)(1+\tau_5 s)}{\{(1+\tilde{\tau}_2 s)(1+\tau_3 s)(1+\tau_4 s)\}^2}\,\frac{1}{vC_n B}\,\frac{1}{1+\left\{\tau_{10} s\,\frac{(1+\tau_6 s)(1+\tau_7 s)}{(1+\tau_3 s)(1+\tau_4 s)}\right\}^2}$$

$$\left.\left\{\bar{F}_1\,\frac{\tau_{10} s\,(1+\tau_6 s)(1+\tau_7 s)}{(1+\tau_3 s)(1+\tau_4 s)} + \bar{F}_2 + \frac{\bar{F}_3}{1+\tau_0 s\,\frac{(1+\tau_6 s)(1+\tau_7 s)}{(1+\tau_3 s)(1+\tau_4 s)}}\right\}\right]$$

$$\cong Q_g(s)\left[\frac{(1-\gamma)}{C_f}\left\{\frac{\bar{B}_3 + \bar{B}_4 s + \bar{B}_5 s^2}{(1+\tilde{\tau}_2 s)(1+\tau_3 s)(1+\tau_4 s)}\right\} + \frac{1}{vC_n B}\right.$$

$$\frac{(1+\tau_8 s)}{(1+\tilde{\tau}_2 s)(1+\alpha_1 s+\alpha_2 s^2+\alpha_3 s^3)}\left\{\frac{(1+\tau_5 s)(\bar{F}_2+\bar{F}_4 s+\bar{F}_5 s^2)}{(1+\tilde{\tau}_2 s)(1+\tau_3 s)(1+\tau_4 s)}\right.$$

$$\left.\left.+\frac{(1+\tau_5 s)\{\bar{F}_3 + \bar{F}_3(\tau_3+\tau_4)s + \bar{F}_3\,\tau_3\,\tau_4 s^2\}}{(1+\tilde{\tau}_2 s)(1+\beta_1 s+\beta_2 s^2)}\right\}\right], \qquad (D.1)$$

where

$$\overline{F}_1 = 1 - \frac{ABL}{2} \cos C \quad ;$$

$$\overline{F}_2 = -\frac{A}{BL} \sin(BL+C) + A \cos C \quad ;$$

$$\overline{F}_3 = \frac{A}{BL} \sin C \quad ;$$

$$\overline{F}_4 = \tau_3 + \tau_4 + \tau_{10} \quad ;$$

$$\overline{F}_5 = \tau_3 \tau_4 + \tau_{10}(\tau_6 + \tau_7) \quad .$$

APPENDIX E

From Eqs. (4.12) and (7.1) through (7.5), the following equations are obtained:

$$\frac{d\theta_n(\chi,s)}{d\chi} + \theta_n(\chi,s)\frac{s}{vC_n}\left\{C_n + \frac{C_t}{1+\frac{C_t s}{H_3}} + \frac{C_c + C_f F(s)}{1+\frac{s}{2\pi R_2 H_2}\{C_c + C_f F(s)\}}\right\}$$

$$= \frac{\gamma \dot{Q}_g(\chi,s)}{vC_n} + \frac{(1-\gamma)\dot{Q}_g(\chi,s)F(s)/vC_n}{1+\frac{s}{2\pi R_2 H_2}\{C_c + C_f F(s)\}} \quad ; \qquad (E.1)$$

$$\theta_t(\chi,s) = \frac{\theta_n(\chi,s)}{1+\frac{C_t s}{H_3}} \quad . \qquad (E.2)$$

By solving Eq. (E.1), $\theta_n(\chi,s)$ is given:

$$\theta_n(\chi,s) = \{\gamma + (1-\gamma)\xi(s)\}\frac{1}{vC_n}\int_0^x \dot{Q}_g(\chi's)\, e^{\zeta(s)(\chi'-\chi)} d\chi' \quad . \qquad (E.3)$$

APPENDIX F

In a way similar to that used in Appendix B, $\bar{\theta}_n(s)$ is calculated:

$$\bar{\theta}_n(s) = \frac{\{\gamma + (1-\gamma)\zeta(s)\}\dot{Q}_g(s)A^2}{vC_nB^2L} \frac{1}{1 + \left\{\frac{\zeta(s)}{B}\right\}^2} \left[\frac{\zeta(s)L}{2}\right.$$

$$- \frac{\zeta(s)\{\sin 2(BL+C) - \sin 2C\}}{4B} - \frac{\sin^2(BL+C) + \sin^2 C}{2}$$

$$\left. + e^{-\zeta(s)L} \sin(BL+C) \sin C + \frac{1 - e^{-\zeta(s)L}\{\cos BL + \frac{\zeta(s)}{B}\sin BL\}}{1 + \left\{\frac{\zeta(s)}{B}\right\}^2}\right]$$

$$+ {}_b\theta_n(bL,s)\, e^{-T_r s} \frac{A}{BL}\{\cos C - \cos(BL+C)\} \quad . \qquad (F.1)$$

$\zeta(s)$ is then simplified:

$$\zeta(s) \simeq \frac{C_t + C_n + C_c + C_f}{C_n v} \frac{s}{(1+\tau_3 s)(1+\tau_4 s)(1+\tau_{13} s)}$$

$$\times \left[1 + s\left\{\tau_{13} + \frac{C_t(\tau_3 + \tau_4 - \tau_{13}) + C_n(\tau_3 + \tau_4) + C_c\tau_1}{C_t + C_n + C_c + C_f}\right\}\right.$$

$$+ s^2\left\{\frac{C_t\tau_3\tau_4 + C_n(\tau_3\tau_4 + \tau_4\tau_{13} + \tau_{13}\tau_3) + C_c\tau_1\tau_{13}}{C_t + C_n + C_c + C_f}\right\}$$

$$\left. + s^3 \frac{\tau_3\tau_4\tau_{13}}{C_t + C_n + C_c + C_f}\right]$$

$$= \frac{C_t + C_n + C_c + C_f}{C_n v} \frac{s\{1 + h_1 s + h_2 s^2 + h_3 s^3\}}{(1+\tau_3 s)(1+\tau_4 s)(1+\tau_{13} s)} \quad , \qquad (F.2)$$

where

$$\tau_{13} = C_t / H_3 \quad ;$$

$$h_1 = \tau_{13} + \frac{C_t(\tau_3 + \tau_4 - \tau_{13}) + C_n(\tau_3 + \tau_4) + C_c\tau_1}{C_t + C_n + C_c + C_f} \quad ;$$

$$h_2 = \frac{C_t\tau_3\tau_4 + C_n(\tau_3\tau_4 + \tau_4\tau_{13} + \tau_{13}\tau_3) + C_c\tau_1\tau_{13}}{C_t + C_n + C_c + C_f} \quad ;$$

$$h_3 = \frac{\tau_3 \tau_4 \tau_{13}}{C_t + C_n + C_c + C_f}$$

Substituting Eqs. (B.6) and (F.2) into Eqs. (F.1) and (7.7) and applying the following relation:

$$e^{-f(s)} \approx \frac{1}{1 + f(s)} \quad , \tag{F.3}$$

gives the power generation rate to the hexagonal tube temperature transfer function

$$\frac{\bar{\theta}_t(s)}{\bar{\dot{Q}}_g(s)} \simeq \frac{\bar{H}_1}{1 + \tau_{13}s} \frac{1 + \tau_8 s}{(1 + \tilde{\tau}_2 s)(1 + \tau_3 s)(1 + \tau_4 s)}$$

$$\frac{1}{1 + \left\{\tau_{14}s \frac{1 + h_1 s + h_2 s^2 + h_3 s^3}{(1 + \tau_3 s)(1 + \tau_4 s)(1 + \tau_{13} s)}\right\}^2}$$

$$\left[-\bar{H}_2 + \bar{H}_3 \frac{s(1 + h_1 s + h_2 s^2 + h_3 s^3)}{(1 + \tau_3 s)(1 + \tau_4 s)(1 + \tau_{13} s)} \right.$$

$$+ \frac{\bar{H}_4}{1 + \tau_{15}s \frac{(1 + h_1 s + h_2 s^2 + h_3 s^3)}{(1 + \tau_3 s)(1 + \tau_4 s)(1 + \tau_{13} s)}}$$

$$+ \frac{1}{1 + \left\{\tau_{14}s \frac{(1 + h_1 s + h_2 s^2 + h_3 s^3)}{(1 + \tau_3 s)(1 + \tau_4 s)(1 + \tau_{13} s)}\right\}^2}$$

$$\left. \left\{ 1 - \frac{\bar{H}_5 + \bar{H}_6 s}{1 + \tau_{15}s \frac{(1 + h_1 s + h_2 s^2 + h_3 s^3)}{(1 + \tau_3 s)(1 + \tau_4 s)(1 + \tau_{13} s)}} \right\} \right]$$

$$+ \frac{{}_b\dot{Q}_g(s)}{\dot{Q}_g(s)} \frac{{}_b\theta_n(sL)}{{}_b\dot{Q}_g(s)} \frac{1}{1 + T_r s} \frac{1}{1 + \tau_{13} s} \quad , \tag{F.4}$$

where

$$\bar{H}_1 = A^2/vC_n LB^2 = \bar{A}_1 \quad ;$$

$$\bar{H}_2 = \{\sin^2(BL + C) + \sin^2 C\}/2 = \bar{A}_2 \quad ;$$

$$\bar{H}_3 = \frac{C_t + C_n + C_c + C_f}{C_n v}\left\{\frac{L}{2} - \frac{\sin 2(BL+C) - \sin 2C}{4B}\right\} ;$$

$$\bar{H}_4 = \sin(BL+C)\sin C = \bar{A}_4 ;$$

$$\bar{H}_5 = \cos BL = \bar{A}_5 ;$$

$$\bar{H}_6 = \frac{C_t + C_n + C_c + C_f}{C_n vB}\sin BL ;$$

$$\tau_{14} = (C_t + C_n + C_c + C_f)/C_n vB ;$$

$$\tau_{15} = (C_t + C_n + C_c + C_f)L/C_n v .$$

By a procedure similar to that in Appendix B [Eq's. (B.10) through (B.12)], Eq. (F.4) can be simplified:

$$\frac{1}{1 + \left\{\tau_{14}s\frac{1 + h_1 s + h_2 s^2 + h_3 s^3}{(1+\tau_3 s)(1+\tau_4 s)(1+\tau_{13}s)}\right\}^2} \simeq \frac{\{1 + (\tau_3+\tau_4)s\}^2(1+\tau_{13}s)^2}{1 + \gamma_1 s + \gamma_2 s^2 + \gamma_3 s^3 + \gamma_4 s^4} ; \tag{F.5}$$

$$\frac{1}{1 + \left\{\tau_{15}s\frac{1 + h_1 s + h_2 s^2 + h_3 s^3}{(1+\tau_3 s)(1+\tau_4 s)(1+\tau_{13}s)}\right\}} \simeq \frac{\{1 + (\tau_3+\tau_4)s\}(1+\tau_{13}s)}{1 + \delta_1 s + \delta_2 s^2 + \delta_3 s^3} . \tag{F.6}$$

Then,

$$\frac{\bar{\theta}_t(s)}{\dot{Q}_g(s)} = \frac{\bar{H}_1(1+\tau_8 s)(1+\tau_{13}s)(1+\tau_3 s)(1+\tau_4 s)}{(1+\tilde{\tau}_2 s)(1+\gamma_1 s+\gamma_2 s^2+\gamma_3 s^3+\gamma_4 s^4)}\left[-\frac{\bar{H}_2 + \bar{H}_7 s + \bar{H}_8 s^2 + \bar{H}_9 s^3}{(1+\tau_3 s)(1+\tau_4 s)(1+\tau_{13}s)}\right.$$

$$+ \frac{\bar{H}_4\{1 + (\tau_3+\tau_4)s\}(1+\tau_{13}s)}{1 + \delta_1 s + \delta_2 s^2 + \delta_3 s^3} + \frac{\{1 + (\tau_3+\tau_4)s\}^2(1+\tau_{13}s)^2}{1 + \gamma_1 s + \gamma_2 s^2 + \gamma_3 s^3 + \gamma_4 s^4}$$

$$\left.\times \frac{1 - \bar{H}_5 + \bar{H}_{10} s + \bar{H}_{11} s^2 + \bar{H}_{12} s^3}{1 + \delta_1 s + \delta_2 s^2 + \delta_3 s^3}\right] + \frac{b\dot{Q}_g(s)}{\dot{Q}_g(s)}\frac{b\theta_n(bL,s)}{b\dot{Q}_g(s)}\frac{1}{1+T_r s}\frac{1}{1+\tau_{13}s} \tag{F.7}$$

where

$$\overline{H}_7 = -\overline{H}_2(\tau_3 + \tau_4 + \tau_{13}) + \overline{H}_3 \quad ;$$

$$\overline{H}_8 = -\overline{H}_2\{\tau_{13}(\tau_3 + \tau_4) + \tau_3\tau_4\} + h_1\overline{H}_3 \quad ;$$

$$\overline{H}_9 = -\overline{H}_2\tau_3\tau_4\tau_{13} + h_2\overline{H}_3 \quad ;$$

$$\overline{H}_{10} = \delta_1 - \overline{H}_5(\tau_3 + \tau_4 + \tau_{13}) - \overline{H}_6 \quad ;$$

$$\overline{H}_{11} = \delta_2 - \overline{H}_5\{\tau_{13}(\tau_3 + \tau_4) + \tau_3\tau_4\} - \overline{H}_6(\tau_3 + \tau_4 + \tau_{13}) \quad ;$$

$$\overline{H}_{12} = \delta_3 - \overline{H}_5\tau_3\tau_4\tau_{13} - \overline{H}_6\{\tau_{13}(\tau_3 + \tau_4) + \tau_3\tau_4\} \quad ;$$

$$\gamma_1 = 2(\tau_3 + \tau_4 + \tau_{13}) \quad ;$$

$$\gamma_2 = (\tau_3 + \tau_4 + \tau_{13})^2 + 2\{(\tau_3 + \tau_4)\tau_{13} + \tau_3\tau_4\} + \tau_{14}^2 \quad ;$$

$$\gamma_3 = 2\{(\tau_3 + \tau_4)\tau_{13} + \tau_3\tau_4\}(\tau_3 + \tau_4 + \tau_{13})\} + 2\tau_{14}^2 h_1 \quad ;$$

$$\gamma_4 = \{(\tau_3 + \tau_4)\tau_{13} + \tau_3\tau_4\}^2 + 2\tau_3\tau_4\tau_{13}(\tau_3 + \tau_4 + \tau_{13}) + \tau_{14}^2(2h_2 + h_1^2) \quad ;$$

$$\delta_1 = \tau_3 + \tau_4 + \tau_{13} + \tau_{15} \quad ;$$

$$\delta_2 = \tau_3\tau_4 + \tau_{13}(\tau_3 + \tau_4) + h_1\tau_{15} \quad ;$$

$$\delta_3 = \tau_3\tau_4\tau_{13} + \tau_{15}h_2 \quad .$$

APPENDIX G

SYMBOLS AND CONSTANTS

Section III

N	Neutron density
ρ	Reactivity
ℓ^*	Mean prompt-neutron lifetime
λ_i	Decay constant of delayed neutrons of group i
C_i	Concentration of delayed neutrons emitted in group i
β_i	Fraction of delayed neutrons emitted in group i

Sections IV and V

θ	Temperature, °C
$\dot{Q}_g$	Power generation rate/unit length
λ_f	Thermal conductivity
k_f	Thermal diffusivity of fuel slug
R_1	Radius of fuel slug
H_1	Effective heat transfer coefficient from fuel slugs to cladding
γ	Fraction of power generation carried by gamma radiation
H_2	Heat transfer coefficient from cladding to coolant
C	Heat capacity/unit length
R_2	Fuel rod radius
L	Axial length of medium
v	Coolant velocity
δ_{Na}, δ_{Zr}	Thickness of NaK bond and Zircaloy jacket
${}_uH_2$	Effective heat transfer coefficient from upper blanket slugs to coolant/unit length
λ_{Na}, λ_{Zr}	Thermal conductivity of NaK and Zircaloy

Section VI

r_1	Displacement of fuel slug due to bowing
α	Thermal expansion coefficient of fuel slug
d	Diameter of fuel slug or upper blanket slug

θ_{df} Temperature difference between the core center side and opposite side of one fuel slug

$\bar{\theta}'_f(s)$ Axially average fuel temperature (does not include the axial importance function)

P_i Steady-state power generation in the case i

P_{im} Maximum steady-state power generation in the case i for satisfying the condition that the fuel slug in the jacket does not touch the jacket wall

Section VII

H_3 Effective heat transfer coefficient from coolant to hexagonal tube/unit length of one rod

R_3 Effective core radius

r_2 Displacement of core due to hexagonal tube thermal expansion

R_4 Effective inner blanket radius

Section VIII

K, ΔK Multiplication factor and its small deviation

K_n Reactivity coefficient of the NaK temperature in the core

K_{nc} Reactivity coefficient of the NaK coolant temperature in the core

K_{f_1} Reactivity coefficient of the fuel temperature due to axial expansion

K_{f_2} Reactivity coefficient of the fuel temperature due to decreases of NaK volume

K_f Reactivity coefficient of the fuel temperature $(K_{f_1} + K_{f_2})$

K_{nb} Reactivity coefficient of the NaK bond temperature in the core

K_{zj} Reactivity coefficient of the jacket temperature due to decreases of NaK volume

K_j Reactivity coefficient of the cladding temperature $(K_{nb} + K_{zj})$

K_d Reactivity coefficient of the core radial displacement

${}_uK_n$ Reactivity coefficient of the NaK coolant temperature in the upper blanket

${}_uK_f$ Reactivity coefficient of the blanket slug temperature in the upper blanket

K_r	Reactivity coefficient of the isothermal reactor temperature due to core radial expansion
${}_lK_n$	Reactivity coefficient of the NaK coolant temperature on the lower blanket
${}_lK_f$	Reactivity coefficient of the blanket slug temperature in the lower blanket
${}_bK_n$	Reactivity coefficient of the NaK coolant temperature in the inner blanket
${}_bK_{f_1}$	Reactivity coefficient of the inner blanket slug temperature due to slug expansion
${}_bK_{f_2}$	Reactivity coefficient of the inner blanket slug temperature due to decreases of NaK volume
${}_uK_r$	Reactivity coefficient of the upper blanket temperature due to its radial expansion
${}_lK_r$	Reactivity coefficient of the lower blanket temperature due to its radial expansion
${}_bK_r$	Reactivity coefficient of the inner blanket temperature due to its radial expansion
K_{it}	Isothermal temperature coefficient
a_n	Cross-section area for coolant flow/rod
a_{nb}	Cross-section area of NaK bond
a_f	Cross-section area of fuel slug
a_j	Cross-section area of Zircaloy jacket

Subscripts

Left subscripts		Right subscripts	
b	Inner blanket	f	Fuel or blanket slug
u	Upper blanket	c	Cladding
non	Core	n	NaK coolant
		t	Stainless steel hexagonal tube

The material constants are listed in Table G.1.

Table G.1

Material Constants

	PuAl	U	NaK	Zircaloy	Stainless Steel
Thermal Conductivity (cal/cm-sec-°C)	0.041	0.07	0.0621	0.0332	-
Density (g/cm^3)	16.3	18.9	0.79	6.55	7.9
Specific Heat (cal/g-°C)	0.0364	0.032	0.2122	0.08	0.12
Thermal Diffusivity (cm^2/sec)	0.0691	0.1157	-	-	-
Thermal Expansion Coefficient	$12.5 \times 10^{-6} \Delta\ell/\ell$	$14 \times 10^{-6} \Delta\ell/\ell$	$3 \times 10^{-4} \Delta V/V$	$9.6 \times 10^{-6} \Delta\ell/\ell$	$18 \times 10^{6} \Delta\ell/\ell$

Constants independent of the coolant flow rate are tabulated in Table G.2.

Table G.2

(A) Geometrical Constant Core

	Core	Upper Blanket	Inner Blanket
L	21.5493	19.6723	50.269
R_1	0.29464	"	0.46228
a_f	0.27273	"	0.67137
a_{nb}	0.06194	"	-
a_j	0.11833	"	0.15566
a_n	0.1768	"	0.2632
R_2	0.37973	"	0.51308
R_3	9.037	"	
R_3/R_4	0.60698		

(B) Non-geometrical Constants

cal/cm	C_t	0.187424				
cal/cm	C_f	0.1618	$_uC_f$	0.2373	$_bC_f$	0.40604
cal/cm	C_c	0.07239			$_bC_c$	0.08157
cal/cm	C_n	0.02964	$_uC_n$	0.02964	$_bC_n$	0.04412
cal/cm^{2}sec°C	H_1	0.4722			$_bH_1$	0.6535
	M	3.3934			$_bM$	4.3157
	T	1.2563			$_bT$	1.8470
	F_1	0.911			$_bF_1$	0.889
	F_2	0.089			$_bF_2$	0.111
	τ_1/T	0.296			$_b\tau_1/_bT$	0.267
	$\tilde{\tau}_2/T$	0.416			$_b\tilde{\tau}_2/_bT$	0.0419
	τ_1	0.372			$_b\tau_1$	0.493
	$\tilde{\tau}_2$	0.0523			$_b\tilde{\tau}_2$	0.0774
	A	1.13358				
	B	0.081944				
	C	0.68790				
	G_2	0.0675				

$\sin(BL+C) = 0.6193$ $\sin C = 0.6349$ $\sin BL = 0.97696$

$\cos(BL+C) = -0.78515$ $\cos C = 0.77259$ $\cos BL = -0.21341$

$\sin^2(BL+C) = 0.38353$ $\sin^2 C = 0.40310$ $\sin 2(BL+C) = 0.97249$

$\sin 2C = 0.98103$